SULAIMANI
Dental Joural

An Open Access Journal Published by the College of Dentistry,University of Sulaimani

ISSN 4656-2309
sdj.univsul.edu.iq

Volume 12
Issue 3
December 2025

Sulaimani

Dental Journal

An Open Access Journal Published by the College of Dentistry, University of Sulaimani

Publication Office: College of Dentistry, University of Sulaimani, Sulaymaniyah, Iraq Tel: +(964) 533270913 - +(964) 7702106211 / P.O. Box: 1124-30 Sulaymaniyah - Iraq
E-mail: sdj@univsul.edu.iq

ISSN: 2309-4656

Volume 12

Issue 3

December 2025

About the Journal

Aim

The Sulaimani Dental Journal (Sulaimani Dent J) is a peer-reviewed, open-access (CC BY-NC-SA 4.0), scientific journal published triannually (in April, August, and December) by the College of Dentistry, University of Sulaimani. The journal aims to disseminate high-quality, evidence-based research that advances knowledge and clinical practice in dentistry and the oral health sciences. The journal serves as a platform for dental professionals, researchers, and academics to share innovations, critical reviews, and scholarly discussions that contribute to the improvement of oral health care locally, regionally, and globally.

Article publication policy and author rights

Research assessment policy

The Sulaimani Dental Journal (SDJ) fully supports the principles of the **San Francisco Declaration on Research Assessment (DORA)**. We recognize the need to improve the ways in which the outputs of scholarly research are evaluated. SDJ emphasizes the value of research based on its scientific content rather than solely on journal-based metrics such as the Journal Impact Factor.

In alignment with DORA, we:

- Evaluate research on its own merits, independent of where it is published.
- Encourage authors to present a full and transparent description of their work.
- Avoid the inappropriate use of journal-based metrics in decisions regarding hiring, promotion, or funding.
- Promote responsible research assessment practices across the academic and research community.

We are committed to fostering a culture of integrity, transparency, and fairness in scholarly publishing.

Scope

The Sulaimani Dental Journal welcomes original research articles, systematic reviews, case reports, clinical studies, and short communications across all disciplines of dentistry and oral health, including but not limited to:

- Dental Materials Science
- Oral Medicine and Pathology
- Oral and Maxillofacial Surgery
- Radiology and Diagnostic Imaging
- Prosthodontics and Implantology
- Restorative and Operative Dentistry
- Endodontics
- Periodontology
- Orthodontics
- Pediatric Dentistry
- Dental Public Health and Epidemiology
- Dental Education and Ethics
- Interdisciplinary and Translational Dental Research
- Basic Dental Sciences

The journal also encourages submissions that explore emerging technologies, artificial intelligence applications in dentistry, and interdisciplinary approaches that bridge dental science with broader health and biomedical fields. All manuscripts undergo a rigorous peer-review process and must adhere to ethical standards, including declarations of originality and disclosure of any AI-assisted content beyond language editing.

Editorial Board

Table of Contents

Volume 12, Issue 3: December 2025

Original Article

Comparison Between the Accuracy of Different AI-Based Cephalometric Analysis and Conventional Manual Analysis

Mohammed A. Mahmood[*1], *Adham A. Abdulrahman*[2], *Anwar A. Amin*[2], *Hadi M. Ismail*[2]

Abstract

Objective: This study compared artificial intelligence-based cephalometric analysis platforms with conventional manual analysis using the Steiner Cephalometric analysis system.

Methods: Three AI online software platforms: WEBCEPH, AssembleCircle Corp, South Korea, CEPHIO, Cephio Sp. Z o.o., Poland, and VOXEL Voxel3Di, United Kingdom, were evaluated using 25 cephalometric radiographs and compared with two manual tracings performed using (Lab Pronto, Blue Sky Plan) for the Steiner Cephalometric analysis system. Independent sample t-test was used to compare the two manual analysis. The Kruskal-Wallis H-test, followed by pairwise comparisons, was used to evaluate differences between AI-based and manual analyses, with significance at $p \leq 0.05$.

Results: No significant discrepancies were found between the two manual analyses. However, the Kruskal-Wallis H-test and pairwise comparisons revealed significant differences between the AI platforms regarding the SNA angle and the U1 to NA angle. Specifically, VOXEL AI analysis differed from WEBCEPH (at $p=0.003$) and CEPHIO (at $p=0.011$) for these measurements.

Conclusions: The findings highlight that while AI platforms such as VOXEL show promising alignment with manual analysis across most measurements, discrepancies, particularly in specific angles, underscore the need for cautious integration and ongoing validation of AI in orthodontic practice. The selection of appropriate AI-based analysis is crucial; however, manual analysis remains the gold standard for cephalometric analysis.

Keywords: *Artificial intelligence, Orthodontics, Diagnosis, Automated cephalometric analysis.*

Submitted: April 20, 2025, Accepted: July 20, 2025, Published: December 1, 2025.

Cite this article as: Mahmood MA, Abdulrahman AA, Amin AA, Ismail HM. Comparison Between the Accuracy of Different AI-Based Cephalometric Analysis and Conventional Manual Analysis. Sulaimani Dent J. 2025;12(3):1-9.

DOI: https://doi.org/10.17656/sdj.10211

1. *Department of Basic Science, College of Dentistry, University of Sulaimani, Sulaimani, Iraq.*
2. *Department of Orthodontics, College of Dentistry, University of Sulaimani, Sulaimani, Iraq.*

** Corresponding author*: *muhammed.mahmood@univsul.edu.iq.*

Introduction

Artificial intelligence (AI) may contribute to improved healthcare quality due to the increased quality of diagnostic methods and the elimination of diagnostic errors in daily medical practice. For a century, cephalometric analysis was introduced to the field of orthodontics and became one of the important tools in diagnostic procedures. Moreover, it has been used to evaluate the treatment procedure and monitor the treatment outcomes[1-4]. Manual tracing using tracing paper or tracing software is the most conventional method to identify landmarks and analyze lateral cephalometric radiographs[5]. Digital analysis appeared, and several programs were introduced to perform the analysis, which led to the speed and the accuracy of cephalometric analysis improving significantly[6]. Although analysis with AI was a big development in orthodontics, supervision is still mandatory in identifying the landmarks[7].

The evolution in the field of cephalometric analysis has been marked by the implementation of artificial intelligence (AI) in analysis processes, which is increasing dramatically[6,7]. Several studies indicated that AI-based analysis is a useful tool for identifying cephalometric landmarks and performing analysis, and its measurement can be trusted for orthodontic diagnosis[5,6,8]. As such, the number of studies confirming the reliability and validity of AI-based analysis is still increasing. One of the apparent advantages of AI-based analysis is its speed, which saves orthodontists time during the examination phase.

The introduction of AI into cephalometric analysis marks a pivotal advancement in the development of diagnostic instruments in orthodontics. Historically, landmark identification was conducted using hand tracing techniques and was regarded as the gold standard for lateral cephalometric research. The emergence of digital analysis has enhanced the efficiency and accuracy of cephalometric evaluations[2]. The automated methods for identifying and analysing cephalometric landmarks represent a significant advancement in cephalometric analysis procedures. They have markedly enhanced efficiency, rendering them progressively appropriate for routine diagnosis in orthodontics[9]. Their improved speed and precision provide significant advantages, indicating a considerable change in the domain. The rising endorsement of daily utilization by orthodontic professionals underscores the escalating importance of these automated techniques in orthodontic practice[10].

The advent of AI-driven cephalometric analysis has resulted in a significant decrease in the time needed for evaluation. Nonetheless, the precision of the research requires further examination, and other studies have emerged in the sector during the past three years. Cephalometry plays a crucial role in orthodontic diagnosis and treatment planning, making the integration of AI a compelling proposition and stimulating research to assess its reliability and usefulness[1]. Furthermore, AI systems can perpetually enhance their capabilities by assimilating new data, rendering them versatile for various craniofacial deformities and heterogeneous patient demographics. This adaptability is essential in orthodontics, where individual anatomical differences greatly influence diagnostic and treatment results. The capacity of AI systems to learn and adapt provides a versatile instrument that can align with the changing clinical requirements and progress in orthodontic research.

Notwithstanding encouraging outcomes, thorough comparative studies are imperative to assess the efficacy of diverse AI-based platforms in relation to conventional manual techniques utilizing standardized systems such as the Steiner Cephalometric analysis system. These studies confirm the validity and dependability of AI systems in various therapeutic contexts and patient populations. By comparing different AI platforms, researchers can identify the most effective systems, guiding orthodontists in selecting the best tools for their practice. Therefore, this study aimed to compare different AI-based cephalometric analysis platforms and compare each of these platforms with conventional manual cephalometric analysis using a definite analysis system (Steiner Cephalometric analysis system).

Materials and methods

The study was approved by the ethical committee of the College of Dentistry at the University of Sulaimani with reference number (CoD-EC-24-004) on August 29, 2024.

Sample Selection

In this observational study, data were retrospectively extracted from lateral cephalometric radiographs of individuals currently undergoing orthodontic treatment, sourced from the patient database of the College of Dentistry, University of Sulaimani. For this study, 25 patients who had undergone lateral cephalometric radiographs between 2021 and 2024 were selected. The G Power software (version 3.1, Heinrich Heine-University Dusseldorf, Germany) was utilized to determine the statistical power, aiming for 80%, at a significance level (alpha) of 0.05 using a two-sided paired t-test. Based on findings from a prior study[12], it was determined that a sample size of 25 images would be sufficient, assuming an effect size of 0.49.

All cephalometric radiographs were obtained using the PaX-I smart (Vatech, Seoul, Korea) with settings of 85 kVp, 10 mA, and an exposure time of 1.2-3.3 seconds.

The same technician took all the radiographs. Patients were in a standing position with the Frankfort plane parallel to the ground, teeth in centric occlusion, and lips relaxed. Inclusion criteria were cephalometric radiographs of patients aged 14-30 years of both sexes, and the radiographs were selected randomly regardless of malocclusion type to maintain generalizability. Exclusion criteria included radiographs with artifacts, prosthetic restorations, and patients with cleft lip, palate, or trauma.

All cephalometric images were exported as JPG files and saved on a computer. Each radiograph was analysed twice using (Lab Pronto and BlueSky Plan) (Figure 1). Tracing was performed directly on the software.

Cephalometric Analysis Systems: Steiner's cephalometric analysis system (Figure 2) serves as the common framework for both AI-based and manual analyses. Three distinct AI-based platforms: WEBCEPH, Assemble Circle Corp, South Korea, CEPHIO, Cephio Sp. z o.o., Poland, and VOXEL Voxel3Di, United Kingdom, were individually employed (Figures 3, 4, and 5). Steiner analysis is available in all three AI-based systems, and ten readings were selected which were present across all platforms. The same quality radiograph was uploaded to all three AI analysis platforms, and the automated digitization was saved without any manual modifications. The next step involved ordering Steiner cephalometric analysis using the predetermined options in the AI analysis systems. Prior to formal data collection, a calibration session was conducted. Ten randomly selected cephalograms were traced by both examiners, and intraclass correlation coefficients (ICC) were calculated to ensure consistency (ICC > 0.9 for all parameters). For AI-based methods, all radiographs were scaled using the embedded reference rulers within each platform prior to analysis.

Manual Analysis: Tracing software was used and the points placed by operators to perform the Steiner system. This conventional method was carried out by two experienced orthodontists, each with a minimum of 15 years of clinical proficiency in cephalometric analysis. Both linear and angular measurements derived from manual and AI-based analyses were accurately considered during the comparative assessment (Table 1).

Landmark Identification and Measurement Process

1. Identification of Landmarks: The following landmarks were identified on each radiograph:
    1. Sella (S): The midpoint of the pituitary fossa.
    2. Nasion (N): The most anterior point on the frontonasal suture.
    3. A Point (A): The deepest point on the contour of the premaxilla.
    4. B Point (B): The deepest point on the contour of the mandible.
    5. Pogonion (Pog): The most anterior point on the chin.
    6. Menton (Me): The lowest point on the mandible.
    7. Gonion (Go): The most posterior-inferior point on the angle of the mandible.
    8. Upper Incisor Tip (U1): The tip of the upper central most protruded incisor.
    9. Lower Incisor Tip (L1): The tip of the lower central incisor.
2. Tracing Landmarks: The identified landmarks were traced on digital images using tracing software. The orthodontists ensured precision by consistently using the same set of landmarks for every analysis.

Statistical Analysis:

Microsoft Excel, IBM SPSS statistical package version 29, and DATAtab Team (2024). DATAtab: Online Statistics Calculator. DATAtab e.U. Graz, Austria, were used to tabulate and analyze the data; the Shapiro-Wilk test was used to test the data's normality. Independent sample t-test was used to show the inter-examiner differences between the two manual tracings. Kruskal-Wallis H-test was used to represent the differences between all groups.

Results

Twenty-five cephalometric radiographs were used in this study, the distribution of the data summarized in Table 1. The radiographs were analyzed by three AI online software programs and manual tracing by two experienced orthodontists. The resulting data was tabulated in Microsoft Excel and analyzed by IBM SPSS Statistics version 29.0.1.0 and DATAtab Team (2024). DATAtab: Online Statistics Calculator. DATAtab e.U. Graz, Austria.

Shapiro-Wilk test showed that the distribution of data in the manual analysis groups was normal. In contrast, for most of the AI analysis, it deviated from normality, and accordingly, the Kruskal-Wallis H-test (non-parametric analysis was used to show differences between the groups. The SNA angle measurement shows significant difference among groups (p-value= 0.007), also U1 to NA(deg) shows significant difference between groups (p-value= 0.002).

The t-test indicates no significant differences between the two manual analyses (Table 2) (t = -0.25, p-value = 1).

Median and interquartile range were calculated for all variables, then the results of the Kruskal Wallis H-test with pairwise comparison between groups were shown. VOXEL and WEBCEPH results were different in the analysis of SNA (p-value= 0.003); also, VOXEL and CEPHIO, and VOXEL and WEBCEPH were significantly different regarding the measurement of U1 to NA angle (p-value= 0.031).

Table 1: Steiner Cephalometric Analysis System.[24]

Measurement	Description
SNA Angle	Angle formed by the SN line and the NA line.
SNB Angle	Angle formed by the SN line and the NB line.
ANB Angle	Angle formed by the NA line and the NB line.
Occlusal Plane to SN Angle	Measures the angle between the occlusal plane and the Sella-Nasion line.
Mandibular plane angle (Go-Gn to SN)	Indicates the vertical relationship between the cranial base and the mandibular plane.
U1-NA Angle	Measures the inclination of the upper incisors relative to the NA line.
U1-NA Linear	Measures the linear distance of the upper incisors to the NA line.
L1-NB Angle	Measures the inclination of the lower incisors relative to the NB line.
L1-NB Linear	Measures the linear distance of the lower incisors to the NB line.
Interincisal Angle	Measures the angle formed by the intersection of the long axes of the upper and lower incisors.

Table 2: Showing the distribution of the study sample (median and interquartile range), and the differences between and within the study groups.

Measurements	VOXEL	WEBCEPH	CEPHIO	Manual 1	Manual 2	Kruskal Wallis Test (p-value)
SNA	79.12 (4.81)^{A}	82.69(2.67)^{B}	80.9(3.5)^{AB}	80(5)^{AB}	80.9(4.2)^{AB}	**0.007**
SNB	74.81(0)	76.99(0.29)	76.8(0.02)	76(0.33)	77.7(0.31)	0.193
ANB	3.94(3.66)	5.97(4.73)	4.3(5.9)	5(5)	4.2(4.5)	0.695
Occlusal plane to SN angle	18.75(5.02)	16.86(7.5)	16(5.6)	14(5)	15.8(5.5)	0.089
Mandibular plane angle (Go-Gn to SN)	33.77(9.44)	32.44(7.31)	34.9(7)	32(7)	34.3(6.9)	0.374
U1 to NA (mm)	4.42(3.62)	3.42(2.23)	4.6(3)	4(3)	4.1(2.6)	0.188
U1 to NA (deg)	27.92(8.31)^{D}	21.29(9.35)^{C}	20.7(9.9)^{C}	28(11)^{CD}	25.8(8.8)^{CD}	**0.002**
L1 to NB (mm)	4.64(3.49)	5.12(4.09)	3.8(5.5)	5(5)	3.9(3)	0.751
L1 to NB (deg)	23.57(10.3)	27.41(7.87)	28.6(11.2)	30(10)	27.9(12)	0.211
Interincisal angle	121.76(21.18)	127.45(19.45)	127.5(17.6)	120(19)	123.7(23.6)	0.152

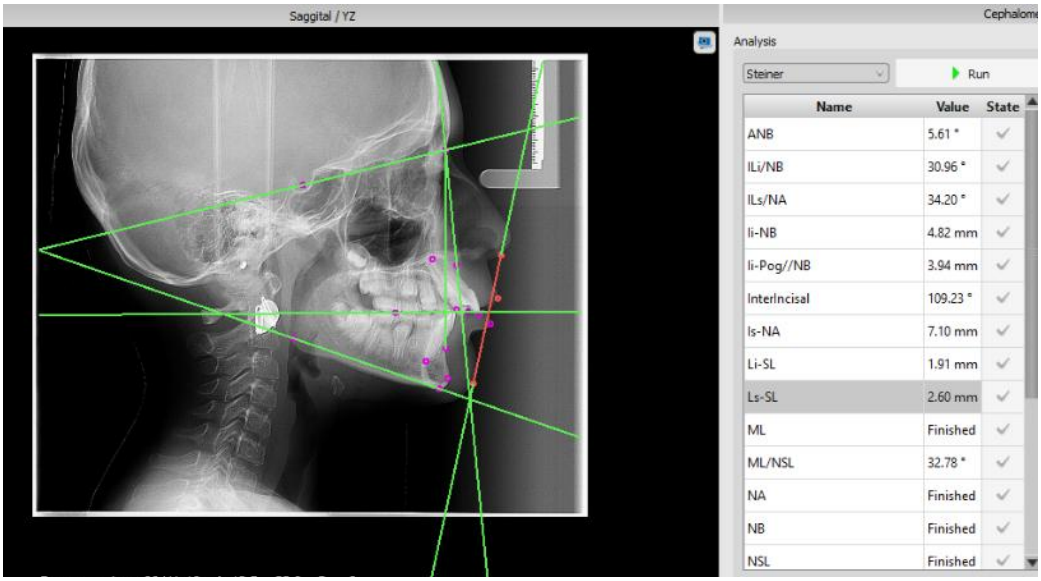

Figure 1: Screenshot of the Steiner analysis by manual analysis using (BlueSky Plan).

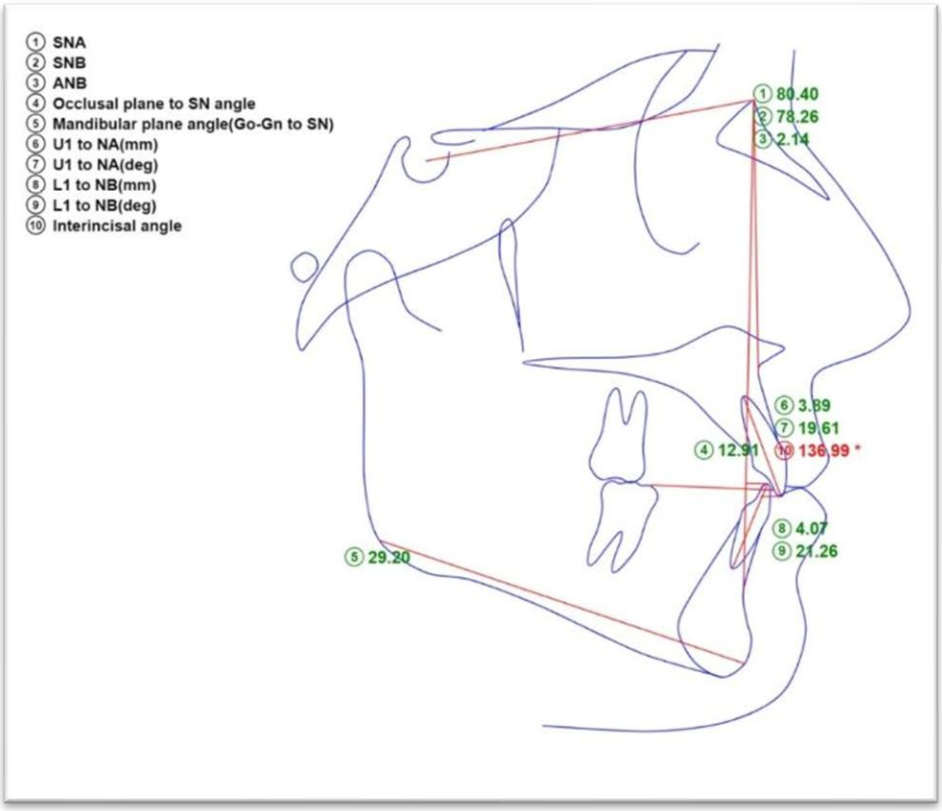

Figure 2: Steiner Analysis Measurements.

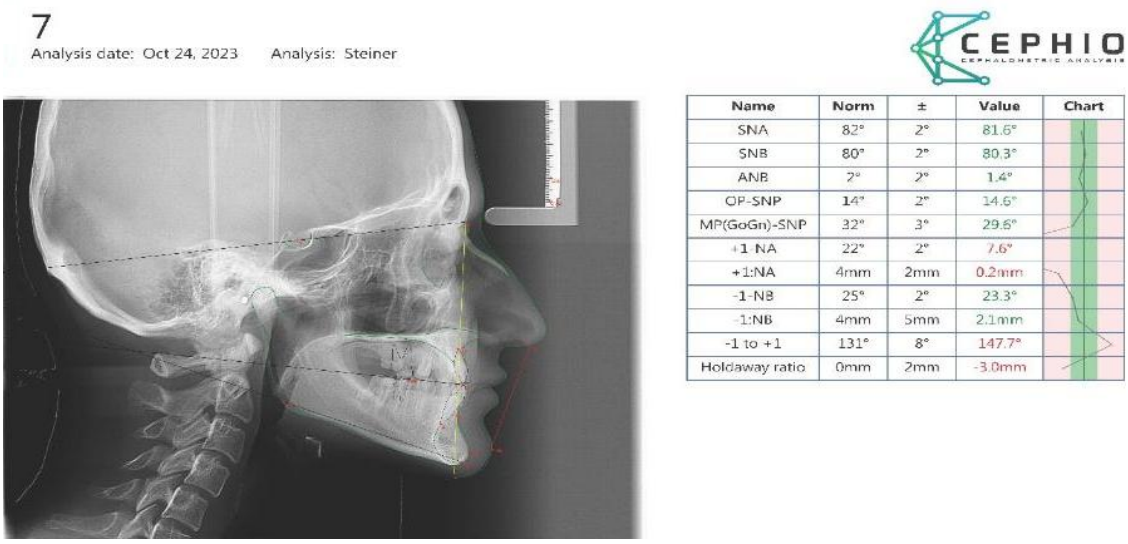

7

Analysis date: Oct 24, 2023 Analysis: Steiner

CEPHIO

Name	Norm	±	Value	Chart
SNA	82°	2°	81.6°	
SNB	80°	2°	80.3°	
ANB	2°	2°	1.4°	
OP-SNP	14°	2°	14.6°	
MP(GoGn)-SNP	32°	3°	29.6°	
+1-NA	22°	2°	7.6°	
+1:NA	4mm	2mm	0.2mm	
-1-NB	25°	2°	23.3°	
-1:NB	4mm	5mm	2.1mm	
-1 to +1	131°	8°	147.7°	
Holdaway ratio	0mm	2mm	-3.0mm	

Figure 3: Screenshot of the CEPHIO analysis system and the output report.

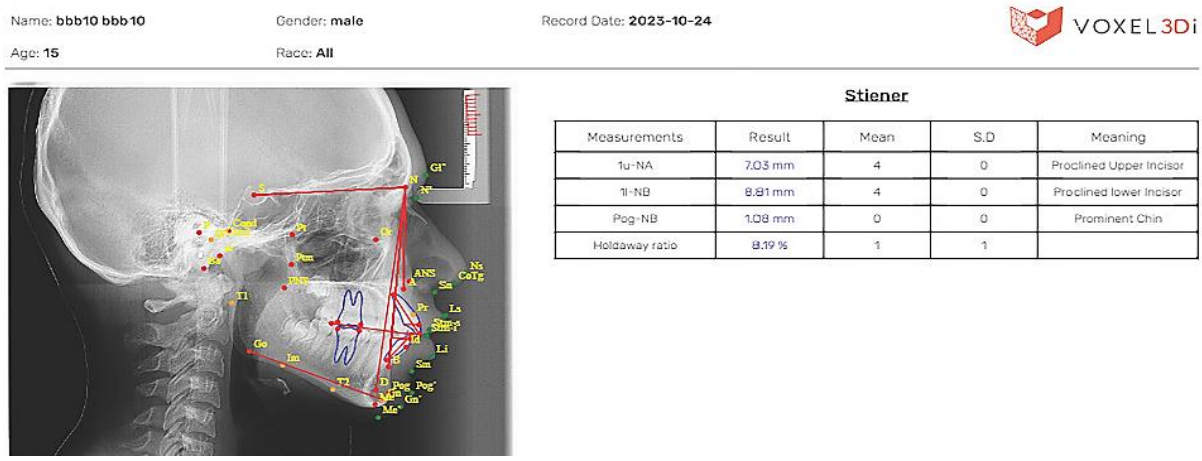

Name: **bbb10 bbb10** Gender: **male** Record Date: **2023-10-24**

Age: **15** Race: **All**

VOXEL 3Di

Stiener

Measurements	Result	Mean	S.D	Meaning
1u-NA	7.03 mm	4	0	Proclined Upper Incisor
1l-NB	8.81 mm	4	0	Proclined lower Incisor
Pog-NB	1.08 mm	0	0	Prominent Chin
Holdaway ratio	8.19 %	1	1	

Figure 4: Screenshot of the VOXEL analysis system and the output report.

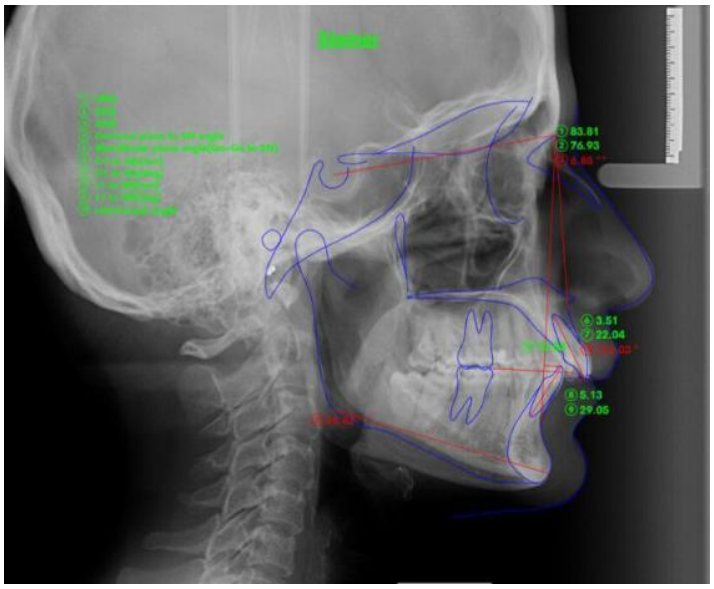

Figure 5: Screenshot of the WEBCEPH analysis system and the readings.

Discussion

This study investigated the accuracy of AI-based Steiner cephalometric analysis by comparing three commercial online systems to manual analysis performed by two experienced orthodontists with extensive expertise in orthodontics and cephalogram tracing. The comparison revealed discrepancies in landmark identification and subsequent angular measurements between the manual tracings and the AI software outputs. These findings highlight inaccuracies within the AI programs, indicating their current limitations in providing reliable cephalometric tracings.

Most of the studies in this regard compared AI analysis with manual or human surveillance analysis to find out the accuracy of such analysis[11,13,14]. These studies generally employed varying quantities of cephalograms for testing and validating the database, ranging from a dozen to a thousand. Additionally, regarding the clinicians involved in manually identifying landmarks, variability was exhibited in their number and levels of clinical experience in cephalometric tracing. However, this study and most other studies comparing manual analysis with AI digitization analysis shared a common finding, accentuating this innovation's advantages of time saving and accuracy.

Although computer science advancements have facilitated the extensive use of computers in cephalometry, resulting in improved accuracy, manual analysis skills are still necessary[15,16]. In addition, Cephalometric imaging software, including popular options like Dolphin Imaging, Blue Sky Plan (this study), and QuickCeph, often involves a manual landmark placement process. In the hands of an experienced clinician, this task typically consumes an average of 10 to 15 minutes per case. Despite the clinician's expertise, the manual placement of landmarks is time-consuming and susceptible to errors[17,18]. This study has found that there are no significant differences between the AI analysis system and the manual system (Table 2), while significant differences between AI systems exist. For example, VOXEL and WEBCEPH analysis showed significant differences in SNA, and with CEPHIO in U1 to NA. This may be due to the differences in landmark identification and reading for the same radiographs. These differences in AI analysis systems for cephalometric analysis come from variations in algorithm types, training data quality, data annotation practices, image preprocessing techniques, training and optimization methods, computational resources, and clinical validation processes. These factors collectively influence the accuracy, reliability, and generalizability of AI systems in orthodontic diagnostics[19].

VOXEL AI analysis showed statistical insignificance compared with other AI analysis. This may partly be due to the Convolutional Neural Network (CNN). A CNN filter is designed to detect specific features within the input data, producing a corresponding feature map that highlights those characteristics. The parallel processing nature of CNNs enables them to efficiently recognize patterns within an input, whether an image or a data sequence. The initial layers typically learn low-level features such as edges, textures, or colours, while deeper layers progressively learn more complex and abstract features.

This parallel feature learning is a fundamental aspect of CNNs. It contributes to their effectiveness in tasks like image recognition, object detection, and various other applications where extracting hierarchical features from input data is essential. Therefore, an average convolutional layer learns from 32 to 512 filters[20,21].

Numerous studies have examined the variability in accuracy among several types of AI algorithms[19,22-25]. This variability has also been reflected in our research, as there were significant differences between the AI systems for some parameters (SNA, and U1 to NA line). At the same time, there were no significant differences between the two manual analyses and the three AI analysis systems.

The principal finding of this study indicates that the AI analysis method is not inherently unreliable but requires refinement across various stages of machine development and training. The outcomes suggest that areas within the AI-based cephalometric analysis process merit further enhancement to boost its reliability and effectiveness.

In parallel, the study's secondary outcome underscores that manual analysis remains the standard method for cephalometric analysis despite being time and resource consuming. This implies that, currently, the traditional manual approach continues to offer a level of precision and dependability that surpasses the capabilities of the AI-based method. The acknowledgment of manual analysis as the benchmark underscores its continued relevance and effectiveness in the field despite the advancements made in AI technologies.

While the study underscored the superior precision of manual analysis compared to AI-based methods, certain limitations persist. For instance, the study's sample size for manual tracing and AI-based analysis was limited.

Furthermore, only two orthodontists conducted the manual analyses, suggesting a potential for bias or limited generalizability of results. It is recommended that future studies address these limitations by increasing the sample size for both manual and AI analyses and involving a larger number of orthodontists to perform manual analyses, enhancing the robustness and reliability of findings.

Conclusion

Orthodontists should be mindful of the limitations and consider AI as a complementary tool rather than solely relying on automated analyses. AI-based analysis undoubtedly saves time and expedites the process. Nevertheless, orthodontists must review the analysis and occasionally adjust landmarks, lines, and planes based on their expertise and contextual information. AI analysis developers must prioritize this flexibility, allowing orthodontists the option to modify and refine analyses within their platforms. This collaboration between AI technology and orthodontic expertise will ensure accurate and tailored treatment plans for patients.

References

1. Tsolakis IA, Tsolakis AI, Elshebiny T, Matthaios S, Palomo JM. Comparing a Fully Automated Cephalometric Tracing Method to a Manual Tracing Method for Orthodontic Diagnosis. J Clin Med. 2022;1:6854.2.

2. Bulatova G, Kusnoto B, Grace V, Tsay TP, Avenetti DM, Sanchez FJC. Assessment of automatic cephalometric landmark identification using artificial intelligence. Orthod Craniofac Res. 2021;24 (Suppl 2):37-42.

3. Mohammed MH, Omer ZQ, Aziz BB, Abdulkareem JF, Mahmood TMA, Kareem FA, Mohammad DN. Convolutional Neural Network-Based Deep Learning Methods for Skeletal Growth Prediction in Dental Patients. J Imaging. 2024;10(11):278.

4. Rauf AM, Mahmood TMA, Mohammed MH, Omer ZQ, Kareem FA. Orthodontic Implementation of Machine Learning Algorithms for Predicting Some Linear Dental Arch Measurements and Preventing Anterior Segment Malocclusion: A Prospective Study. Medicina (Kaunas). 2023;59(11):1973.

5. Meriç P, Naoumova J. Web-based Fully Automated Cephalometric Analysis: Comparisons between App-aided, Computerized, and Manual Tracings. Turk J Orthod. 2020;33(3):142-9.

6. Narkhede S, Rao P, Sawant V, Sachdev SS, Arora S, Pawar AM, Reda R, Testarelli L. Digital versus Manual Tracing in Cephalometric Analysis: A Systematic Review and Meta-Analysis. J Pers Med. 2024;14(6):566.

7. Polizzi A, Leonardi R. Automatic cephalometric landmark identification with artificial intelligence: An umbrella review of systematic reviews. J Dent. 2024;146:105056.

8. Guinot-Barona C, Alonso Pérez-Barquero J, Galán López L, Barmak AB, Att W, Kois JC, Revilla-León M. Cephalometric analysis performance discrepancy between orthodontists and an artificial intelligence model using lateral cephalometric radiographs. J Esthet Restor Dent. 2024;36(4):555-65.

9. Jiang F, Guo Y, Yang C, Zhou Y, Lin Y, Cheng F, et al. Artificial intelligence system for automated landmark localization and analysis of cephalometry. Dentomaxillofac Radiol. 2023;52(1):20220081.

10. Wang CW, Huang CT, Lee JH, Li CH, Chang SW, Siao MJ, et al. A benchmark for comparison of dental radiography analysis algorithms. Med Image Anal. 2016;31:63-76.

11. Çoban G, Öztürk T, Hashimli N, Yağci A. Comparison between cephalometric measurements using digital manual and web-based artificial intelligence cephalometric tracing software. Dental Press J Orthod. 2022;27(4):222112.

12. Abdullah RT, Kuijpers MA, Bergé SJ, Katsaros C. Steiner cephalometric analysis: predicted and actual treatment outcome compared. Orthod Craniofac Res. 2006;9(2):77-83

13. Faul F, Erdfelder E, Lang AG, Buchner A. G*Power 3: a flexible statistical power analysis program for the social, behavioral, and biomedical sciences. Behav Res Methods. 2007;39(2):175-91.

14. Jeon S, Lee KC. Comparison of cephalometric measurements between conventional and automatic cephalometric analysis using convolutional neural network. Prog Orthod. 2021;22(1):14.

15. Mahto RK, Kafle D, Giri A, Luintel S, Karki A. Evaluation of fully automated cephalometric measurements obtained from web-based artificial intelligence driven platform. BMC Oral Health. 2022;22(1):132.

16. Hlongwa P. Cephalometric analysis: manual tracing of a lateral cephalogram. South African Dent J. 2019;74(6):318-22.

17. Bao H, Zhang K, Yu C, Li H, Cao D, Shu H, et al. Evaluating the accuracy of automated cephalometric analysis based on artificial intelligence. BMC Oral Health. 2023;23(1):191.

18. Wang CW, Huang CT, Hsieh MC, Li CH, Chang SW, Li WC, et al. Evaluation and Comparison of Anatomical Landmark Detection Methods for Cephalometric X-Ray Images: A Grand Challenge. IEEE Trans Med Imaging. 2015;34(9):1890-900.

19. El-Fegh I, Galhood M, Sid-Ahmed M, Ahmadi M. Automated 2-D cephalometric analysis of X-ray by

image registration approach based on least square approximator. Annu Int Conf IEEE Eng Med Biol Soc. 2008;2008:3949-52.

20. Kiełczykowski M, Kamiński K, Perkowski K, Zadurska M, Czochrowska E. Application of Artificial Intelligence (AI) in a Cephalometric Analysis: A Narrative Review. Diagnostics (Basel). 2023;13(16):2640.

21. François-Lavet V, Henderson P, Islam R, Bellemare MG, Pineau J. An introduction to deep reinforcement learning. Foundations and Trends® in Machine Learning. 2018;11(3-4):219-354.

22. Brownlee J. Deep learning for computer vision: image classification, object detection, and face recognition in python. Machine Learning Mastery; 2019.

23. Leonardi R, Giordano D, Maiorana F. An evaluation of cellular neural networks for the automatic identification of cephalometric landmarks on digital images. J Biomed Biotechnol. 2009;2009:717102.

24. Tanikawa C, Yamamoto T, Yagi M, Takada K. Automatic recognition of anatomic features on cephalograms of preadolescent children. Angle Orthod. 2010;80(5):812-20.

25. Lindner C, Wang CW, Huang CT, Li CH, Chang SW, Cootes TF. Fully Automatic System for Accurate Localisation and Analysis of Cephalometric Landmarks in Lateral Cephalograms. Sci Rep. 2016;6:33581.

26. Park JH, Hwang HW, Moon JH, Yu Y, Kim H, Her SB, Srinivasan G, Aljanabi MNA, Donatelli RE, Lee SJ. Automated identification of cephalometric landmarks: Part 1-Comparisons between the latest deep-learning methods YOLOV3 and SSD. Angle Orthod. 2019;89(6):903-9.

Original Article

Incorporation of Bioactive Glass Nanoparticles in 3D-Printed Acrylic Resin: Impact on Mechanical and Physical Properties: An In Vitro Study

Chawan M. Qader [1*], *Neda Al-Kaisy*[1]

Abstract

Objective: This study aimed to evaluate the effect of incorporating bioactive glass (BAG) nanoparticles at varying concentrations on the mechanical and physical properties of 3D-printed denture base resin. Specifically, flexural strength, surface roughness, and surface hardness.

Methods: Six groups of 3D-printed acrylic resin specimens were studied: one control group (0% BAG) and five experimental groups containing 1%, 1.5%, 2%, 2.5%, and 3% BAG nanoparticles by weight. Flexural strength, surface hardness, and roughness testing were done on 10 specimens. All were digitally planned and 3D printed using SprintRay. XRD, FTIR-ATR, and FESEM were used to characterise the sample. Mechanical testing includes three-point bending for flexural strength, Shore D durometers for surface hardness, and portable roughness testers for surface roughness.

Results: Flexural strength did not differ significantly among groups (ANOVA, $p = 0.527$), with mean values ranging from 130.6 ± 2.4 MPa (control) to 135.5 ± 2.0 MPa (3% BAG). Surface hardness showed significant improvements at 1.5% (89.9 ± 1.2) and 2% (89.9 ± 1.2) compared with the control (88.2 ± 1.6; $p = 0.028$ and $p = 0.020$, respectively). Surface roughness decreased progressively with BAG addition, and the 3% group (0.063 ± 0.017 µm) was significantly smoother than both the control (0.134 ± 0.090 µm; $p = 0.01$) and the 1% group (0.125 ± 0.101 µm; $p = 0.014$).

Conclusions: Incorporating up to 3% BAG nanoparticles into 3D-printed denture base resin can improve surface properties without compromising flexural strength. The concentration between 1.5% and 3% significantly increased the surface hardness and roughness. These advancements imply that BAG-modified resins have the potential to provide advantages such as enhanced clinical longevity and ease of use for prosthetic devices that are manufactured using 3D technology.

Keywords: *Bioactive glass materials, Nanoparticles, Three-dimensional printing, 3D acrylic resin.*

Submitted: August 24, 2025, Accepted: October 9, 2025, Published: December 1, 2025.

Cite this article as: Qader CM, Al-Kaisy N. Incorporation of Bioactive Glass Nanoparticles in 3D-Printed Acrylic Resin: Impact on Mechanical and Physical Properties: An In Vitro Study. Sulaimani Dent J. 2025;12(3):10-20.

DOI: https://doi.org/10.17656/sdj.10212

1. *Department of Prosthodontics, College of Dentistry, University of Sulaimani, Sulaimani, Iraq.*

* *Corresponding author*: *chawan.qadir@univsul.edu.iq.*

Introduction

Three-dimensional (3D) printing is an innovative additive manufacturing method that has been integrated into the dental field, particularly affecting dental esthetics. It enables the production of accurate, comfortable, and aesthetically pleasing prostheses, improving patient outcomes. The adoption of 3D printing in dentistry is gradually increasing due to advantages including diminished production time and costs when compared to the conventional heat-cured acrylic procedure[1,2]. As the demand for chair-side fabrication and same-day delivery of prosthetic appliances increases, it is likely that optimization of printable materials can decrease the use of conventional methods and improve the accessibility of dental care[3].

However, 3D-printed materials often fail to exhibit the mechanical properties of heat-cured PMMA, despite their potential for increased production efficiency and customization. Conventional PMMA exhibited improved flexural strength, impact resistance, and bonding properties[4]. These findings suggest that further development of 3D-printed acrylic resins is necessary to enhance their mechanical and physical properties. Recent comparative work has also shown that 3D-printed denture bases can achieve significantly higher retention values than conventional PMMA bases, emphasizing the functional benefits of additive manufacturing[5].

Nanotechnology has also drawn attention because it is being used to enhance dentistry, particularly in the development of polymer-based products. Nanoparticles are microscopic in size with a large surface area; thus, they can essentially alter the surface and mechanical properties of polymers. The addition of nanofillers to PMMA influences parameters such as bending strength, surface texture, and hardness of the material[6-8].

The incorporation of various nanoparticles and compounds enhances the mechanical and biological properties of the 3D-printed dental acrylic polymers. The best materials to have been used were zirconium dioxide, titanium dioxide, and silver-loaded mesoporous silica nanoparticles. The titanium dioxide nanoparticles increased flexural strength and surface hardness and reduced solubility. Furthermore, they exhibited antifungal efficiency against Candida albicans, especially at doses between 0.10 and 0.50 wt%[9,10]. Zirconium dioxide nanoparticles resulted in enhanced diametral compressive strength, concurrently inducing a reduction in tensile strength, indicating a change in the material's mechanical properties[11]. Silver-loaded mesoporous composites improved surface hardness and crack resistance, and showed potent antifungal activity against *Candida albicans* without significant cytotoxicity[12]. The findings indicate that nanoparticle reinforcement can be utilized to enhance the strength of denture base materials and impart antimicrobial properties.

The performance of these nanofillers is highly affected by concentration, dispersion quality, and surface functionalization. Improvements in mechanical and biological properties may lead to trade-offs, such as alterations in surface roughness and considerations of cytotoxicity[13].

Bioactive glass is regarded as one of the currently available nanomaterials due to its potential bioactivity and clinical advantages. It enhances soft tissue integration, exhibits antimicrobial properties, and promotes bone repair[14]. The controlled dissolution of bioactive glass and the subsequent release of ions can initiate the formation of a hydroxyapatite (HA) layer, which can chemically adhere to living tissues.[15] The extent of this bioactivity is significantly affected by the material's composition and morphology[16,17]. Although these effects were not investigated in the present study, incorporating BAG into 3D-printed resins represents an initial step toward developing biofunctional denture base materials.

To date, BAG has been integrated into composites, glass ionomer cements, and toothpastes,[18] and more recently into 3D printing resins for orthodontic aligners and intraoral devices, where it maintained mechanical strength and exhibited beneficial ion release and biocompatibility[19,20].

However, only a few studies have examined its incorporation into 3D-printed denture base resins, particularly in comparison with conventional heat-cured acrylic resins[20-22]. To the best of our knowledge, the mechanisms by which bioactive nanoparticles interact with 3D-printed acrylic denture bases remain unclear. While the reinforcing effects of bioactive glass have been documented in conventional heat-cured PMMA systems, their incorporation into 3D-printed denture base resins has yet to be comprehensively investigated. This distinction is clinically essential because 3D-printed resins differ in polymerization method and microstructure from conventional PMMA, which may influence nanoparticle interactions and function[23]. Given the growing use of 3D printing in denture manufacturing, it is crucial to assess whether additive manufacturing materials can gain advantages from the incorporation of bioactive glass (BAG).

Therefore, the current study investigates the effect of five different amounts of bioactive glass nanoparticles on the strength, roughness, and hardness of 3D-printed denture base materials. The objective is to determine whether these modifications lead to significant changes

in performance, thereby testing the null hypothesis that they do not.

Materials and methods

Bioactive glass nanoparticle

Bioactive glass nanoparticles (Nanochemazone™, Canada), a GMP and ISO 9001:2015 holding, and Series No. NCZ-RK-243/1224A with a lot size of 300 kg and purity of >99%, a particle size of approximately 100 nm, and a specific surface area ranging from 150 m^2/g, as determined by BET analysis. The composition included SiO_2 (45–55 wt%), CaO (20–30 wt%), Na_2O (10–15 wt%), and P_2O_5 (4–6 wt%), with trace elements ranging from 0.5 to 1 wt%. The bulk density was documented as 1.5 g/cm^3, and the powder exhibited a white to off-white color. This material is certified for dental and bone tissue engineering applications, ensuring biocompatibility.

The study's experimental design

The sample size was calculated using G*Power 3.1 software for a one-way ANOVA (fixed effects, omnibus, one-way), with a significance level (α) of 0.05 and a desired power (1–β) of 0.80. Based on these parameters, the study was powered to detect a medium-to-large effect size (Cohen's $f = 0.335$). A total of 120 specimens were produced via 3D printing, including one control group with pure resin and five experimental groups containing varying concentrations of BAG nanoparticles (1%, 1.5%, 2%, 2.5%, and 3% by weight).

Mixing bioactive glass nanoparticles with 3D acrylic resin

The denture base material used in this study was NextDent 3D printing resin (Vertex Dental, Netherlands). The bioactive glass nanoparticle content was calculated using the known density of liquid NextDent resin (1.20 g/cm^3) to ensure accurate and consistent weight proportions. For a fixed resin volume of 100 cm^3, the total mass was determined to be 120 g. Target concentrations were achieved by applying standard weight percentage formulas to calculate the precise mass of nanoparticles required for each group. Then the resin was manually stirred for 10 minutes in a 400 mL beaker (IWAKI Pyrex®, Japan), followed by the addition of a pre-weighed concentration of nanoparticles measured with a KERN measuring scale (KERN®, Germany) and an ADAM Nimbus scale (Adam Equipment®, USA) with a precision of 0.01 mg (Table 1). The dispersion of nanoparticles is achieved using sonication and vacuum mixing, as effective distribution has been shown to influence the mechanical properties of acrylic nanocomposites[23]. The blend was sonicated for 2 minutes using a Qsonica sonicator (Qsonica, Newtown, CT, USA), stirred for 5 minutes, and then sonicated again for 1 minute. A final five-minute mixing cycle was performed using a Vacuum Power Mixer Plus (Whip Mix, Euro-Vac, USA) to ensure the reproducibility of the preparation method.

While mixing the 3D printing resin with bioactive glass nanoparticles, aluminum foil was used to protect it from ambient light, thereby preventing premature polymerization.

3D-printed denture base resin specimen fabrication

Three-dimensional (3D) model specimens were designed using the Blender for Dental software program (Blender Foundation®), according to ISO 20795-1:2013. Two bar sets were used in the study: 65 × 10 × 3.3 mm for flexural strength testing and 12 × 12 × 3 mm for surface roughness and hardness testing (Fig. 1). The finalized designs were saved as STL (Standard Tessellation Language) files, sliced with adjusted settings, and then exported to the 3D printer.

The samples were printed using a 3D printer (SprintRay®, model SRP2110C). Printing was performed in Turbo mode according to the manufacturer's instructions, using a 100 µm layer thickness and a curing time of 1.5–2 seconds per layer. All samples were printed simultaneously on a single build platform under identical conditions at room temperature for approximately eight minutes.

After the printing process was completed for all of the specimens, they were transferred to the SprintRay Washing Machine. After washing for five minutes in isopropyl alcohol at a concentration of 99%, they were allowed to dry for ten minutes. The final step involved curing the samples under 405 nm blue light in the SprintRay ProCure 2 Curing Machine within 15 minutes. All operations were performed in a setting maintained at 23 ± 2°C and 50 ± 10% relative humidity.

The printed specimens were then manually polished under dry conditions using silicon carbide sandpapers of grits of 400, 600, 800, 1000, and 1500. The application of the individual grits was performed ten times for each grit, and the same operator carried out all finishing operations to ensure standardization. The dimensions of the final samples were checked with a digital caliper to an accuracy of ± 0.1 mm.

Characterization of the specimens

X-Ray Diffraction (XRD) analysis

X-ray diffraction (XRD) examination was performed using an X'Pert PRO diffractometer (Panalytical, Netherlands) equipped with a copper anode, operated at 40 kV and 40 mA. Scanning took place over a 2θ range of 5.01° to 79.97°, utilizing a step size of 0.026°. Diffraction patterns were generated for pure BAG nanoparticles and 3D-printed acrylic resin comprising 3 wt% BAG. The 3% concentration was selected because it showed the most significant nanoparticle mixing in the tested groups, which is optimal for recognizing distinct diffraction peaks and monitoring the dispersion of bioactive glass throughout the resin. The primary purpose of this research was to determine the crystalline phases present and to analyze whether the nanoparticles maintained their structural integrity post-incorporation. The test enabled the determination of crystallite size (D) using the Scherrer equation, which revealed the physical properties of the implanted particles.

Fourier Transform Infrared spectroscopy with Attenuated Total Reflectance (FTIR-ATR)

Fourier Transform Infrared spectroscopy with Attenuated Total Reflectance (FTIR-ATR) was performed with a Spectrum Two spectrometer (PerkinElmer Inc., USA). The investigation was done over the range of 4000–400 cm^{-1} to identify the functional groups contained in the bioactive glass nanoparticles. Specimens were positioned directly on the ATR crystal, and spectra were obtained to reveal the specific vibrational bands associated with silicate-based materials for pure BAG nanoparticles and 3D-printed acrylic resin comprising 3 wt% BAG.

Field Emission Scanning Electron Microscope (FESEM)

Applying a Field Emission Scanning Electron Microscope (ZEISS Sigma VP, Germany) with a spatial resolution of approximately 1.5 nm, the surface morphology and nanoparticle distribution were investigated. One specimen from each group was chosen for imaging. To improve conductivity, a sputter coater was employed to apply a thin gold coating (approximately 20 μm). Under an accelerating voltage of 15 kV, micrographs were captured at magnifications ranging from 2000× to 5000×.

Mechanical tests of specimens

Flexural strength test

For evaluating flexural strength, a total of 60 specimens (ten per group) were prepared. Testing was carried out using a three-point bending setup on a Universal Testing Machine (Cussons, England) with a 50 mm span and a 5 kN load applied at a crosshead speed of 5 mm/min[24]. The diameter of the support was 3.2 mm. The flexural strength (σ) was determined in megapascals (MPa) using the standard formula, and the maximal load at fracture was recorded in Newtons (N).

$$\sigma = \frac{3FL}{2bd^2}$$

The fracture load is denoted by F in Newtons, the span length between supports is L in millimeters (50 mm), the specimen width is b in millimeters, and the specimen thickness is d in millimeters.

Surface roughness test

Surface roughness was measured using a portable tester (SRT-6200, Guangzhou Landtek Instruments Co., Ltd., China)[25]. The device recorded the surface irregularities on an 11 mm trace length. Measurements of three actions were taken in different directions on each specimen, and the mean value was recorded in micrometers (μ).

Surface hardness test

Surface hardness was measured using a digital Shore D durometer[26]. Tests were conducted using a conical indenter (SR 0.1 mm, 30) with a constant load of 44.5 N. For each specimen, measurements were taken at three points, each 2 mm in diameter, around the center. The mean had been taken as the total Shore D hardness value.

Statistical analysis

Data analysis was done using SPSS 25 (IBM Corp., Armonk, NY, USA). To determine whether the specimens followed a normal distribution, the Shapiro-Wilk test was performed. The result indicated that flexural strength and surface hardness data were normally distributed. Resting on this result, one-way analysis of variance (ANOVA) was used to compare the groups, and pairwise comparisons were implemented with the Tukey HSD post hoc test to determine statistical differences. Nonetheless, the results on surface roughness failed to align with the concept of normality.

Hence, instead of the parametric ANOVA, the non-parametric Kruskal-Wallis test was applied to compare the groups, followed by the Mann-Whitney U test for pairwise comparisons. A significant level of $p < 0.05$ was considered for all statistical tests.

Results

Characterization results

X-Ray Diffraction (XRD) analysis

The structural characteristics of pure BAG nanoparticles were identified, and their addition to a 3D-printed acrylic resin matrix containing 3% BAG was examined using XRD analysis. The diffractogram of the pure BAG (Figure 1A) showed a broad hump centered at $2\theta \approx 31.5°$, along with low-intensity broad peaks between 20° and 36°, indicative of an amorphous structure typical of bioactive glass. Minor crystalline reflections at approximately $2\theta \approx 26.5°$ indicate the presence of unreacted crystalline phases most likely arising during precursor materials or partial devitrification.

The X-ray diffraction pattern of composite resin with 3% BAG (Figure 1B) shows sharp peaks at 2θ values of 26.6°, 28.7°, and 31.1°, with the peak at 28.7° exceeding 7000 counts. Narrow full-width at half maximum (FWHM) readings and elevated peak intensities signify an increased level of crystallinity. This indicates that the BAG nanoparticles were effectively integrated into the resin matrix without structural deterioration. The appearance of crystalline characteristics may indicate partial crystallization or structural reorganization of the BAG particles, which can be triggered by thermal or photopolymerization conditions during 3D printing and post-curing.

Fourier Transform Infrared Spectroscopy (FTIR-ATR)

The analysis of BAG nanoparticles by FTIR-ATR (Fig. 2A) showed distinctive absorption bands indicative of their functional groups and structural composition. A significant signal at 3430.76 cm^{-1} implies O–H stretching, indicating the presence of surface hydroxyl groups or moisture. The band at 2925.69 cm^{-1} was ascribed to C–H stretching, presumably from residual organics. A peak at 1650.54 cm^{-1} corresponds to H–O–H bending, indicating the presence of adsorbed water.

A distinct band at 1032.32 cm^{-1}, associated with Si–O–Si asymmetric stretching, verified the silicate framework. The bending modes of Si–O–Si and Si–O, respectively, were shown to be responsible for the supplementary peaks that were observed at 733.08 cm^{-1} and 495.07 cm^{-1}, respectively. A slight rise at 2345.88 cm^{-1} may indicate the presence of carbonate species or ambient carbon dioxide. The spectrum confirmed the characteristic silicate structure of bioactive glass and structural integrity.

The spectrum obtained from FTIR-ATR of 3D-printed acrylic resin modified with BAG nanoparticles (Fig. 2B) exhibited characteristic peaks of both the nanoparticles and the resin. A prominent band at 3434.73 cm^{-1} signified O–H stretching, whereas peaks at 2957.09, 2925.05, and 2854.57 cm^{-1} were attributed to C–H stretching from PMMA. The C=O stretching band was observed at 1730.66 cm^{-1}, while a peak at 1632.72 cm^{-1} indicated H–O–H bending, indicating the presence of adsorbed moisture.

The characteristic peaks of both the resin and the glass were observed in the FTIR-ATR spectrum of the 3D-printed acrylic resin modified with BAG nanoparticles (Fig. 3B). Although three maxima at 2957.09, 2925.05, and 2854.57 cm^{-1} were attributed to C–H stretching in PMMA, a broad band at 3434.73 cm^{-1} was an indication of O–H stretch. The C=O stretching band was seen at 1730.66 cm^{-1}, and a peak representing H–O–H bending (indicative of adsorbed moisture) was seen at 1632.72 cm^{-1}.

Notably, absorption bands between 1250 and 1115 cm^{-1} and in the 700–500 cm^{-1} range confirmed the presence of Si–O–Si and Si–O vibrations from the BAG network. These findings indicate the successful integration of BAG into the resin without altering the polymer's structure.

Field Emission Scanning Electron Microscope (FESEM)

The control group had a homogeneous surface composition, with no nanoparticles present on the surface (0% BAG). In BAG-modified specimens, surface morphology exhibited variation with concentration. At a concentration of 1%, nanoparticles were uniformly distributed with minimal evidence of agglomeration. The 1.5% and 2% groups showed the most advantageous distribution, characterized by uniform dispersion and negligible clustering. While distinct localized aggregations formed at 2.5% and 3%, they were limited in scope and did not significantly impact the overall homogeneity of the composite resin structure. The findings indicate that BAG concentrations of up to 3% can be efficiently integrated into the resin matrix with minimum agglomeration, preserving structural integrity and distribution quality.

The control group (0% BAG): A smooth, uniform surface that lacks any particulate matter.

1% BAG: The nanoparticle distribution is inadequate yet detectable.

1.5% BAG: Particles that are well-dispersed and have optimal integration throughout the matrix.

2% BAG: A homogeneous dispersion with little agglomeration and well-integrated particles.

2.5% BAG: Onset of small localized aggregation.

3% BAG: Clustering is evident in the early stages; however, agglomeration is limited and does not significantly alter the matrix structure.

Flexural strength

The groups with different amounts of bioactive glass did not exhibit statistically significant changes in flexural strength ($p = 0.527$). The average flexural strength varied from 130.45 ± 2.43 MPa in the control group to 135.45 ± 2.01 MPa in the 3% BAG group, with intermediate values obtained for the remaining concentrations. The comprehensive range among all groups ranged from 126.0 to 139.0 MPa (Table 2).

A slight increase in mean flexural strength was observed with increasing BAG concentrations, particularly in the 1.5% and 3% groups; however, these differences did not reach statistical significance.

Surface hardness

The mean and standard deviation of surface hardness values for all acrylic sample groups are summarized in Table 3.

While no overall statistically significant difference in surface hardness was found among the groups ($p > 0.05$), Group C (1.5%, 89.87 ± 1.20) and Group D (2%, 89.93 ± 1.15) showed significantly higher hardness compared to the control group (88.18 ± 1.57), with p-values of 0.028 and 0.020, respectively. None of the other group comparisons was found to be statistically significant. The most significant improvements in surface hardness occurred at concentrations of 1.5% and 2% bioactive glass.

Surface roughness

The mean and standard deviation of surface roughness values for all acrylic sample groups are presented in Table 4. Whereas the Kruskal-Wallis test revealed no statistically significant overall difference in surface roughness between the groups ($H = 10.686$, $p = 0.058$), a trend of decreasing surface roughness with increasing concentration of BAG nanoparticles was identified. Pairwise comparisons revealed significantly lower surface roughness in Group F (3%) compared to both Group A (0%) ($p = 0.010$) and Group B (1%) ($p = 0.014$). Group E (2.5%) also exhibited a reduction in roughness compared to the control; however, the difference was not statistically significant ($p = 0.064$). Incorporating 3% BAG nanoparticles significantly enhances surface smoothness in 3D-printed acrylic resin.

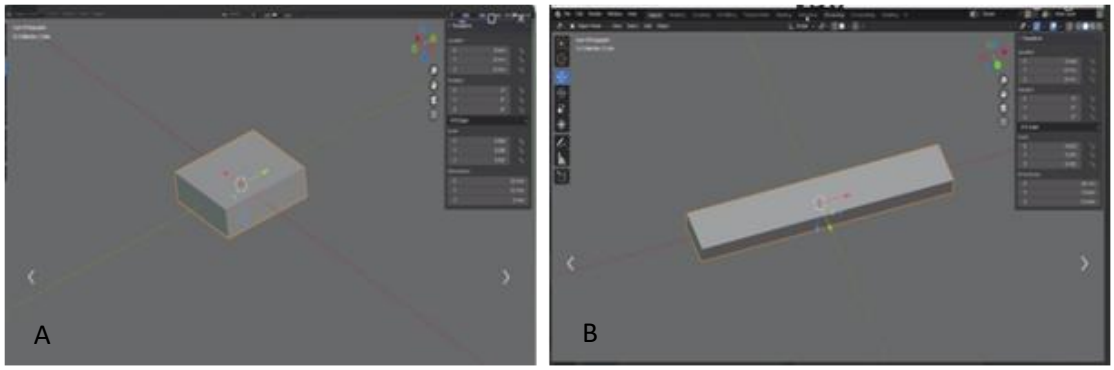

Figure 1: Screenshot of Blender software for flexural strength, surface roughness, and hardness testing, prepared for 3D printing. (A) Design of the sample used for surface roughness and hardness tests. (B) Design of the sample used for flexural strength testing.

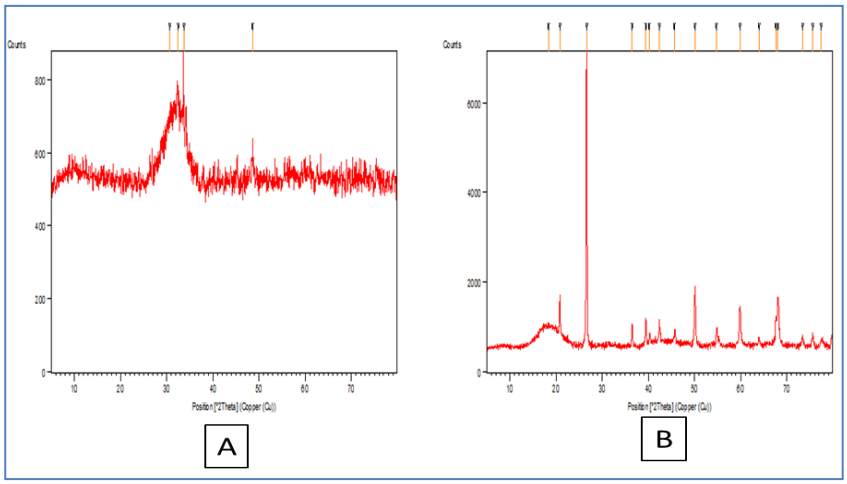

Figure 2: XRD study of BAG nanoparticles (A) and BAG-modified 3D printed acrylic resin (B).

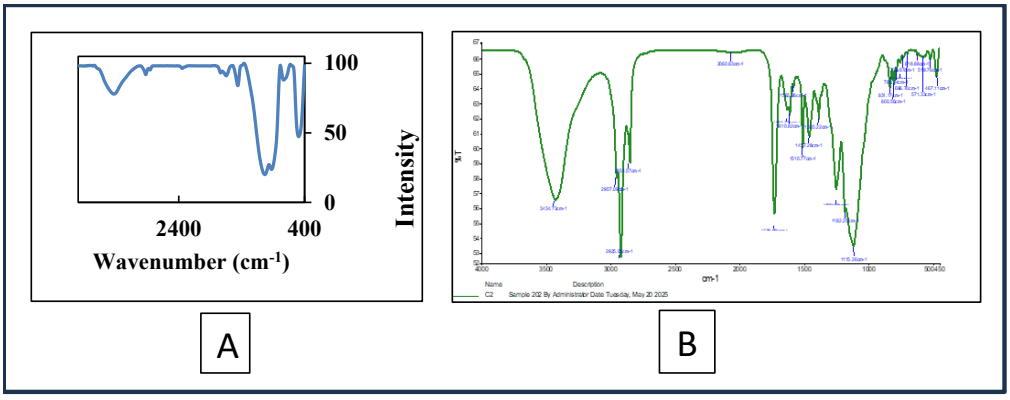

Figure 3: FTIR Spectrum of (A) BAG nanoparticles. FTIR spectrum of (B) BAG mixed with 3D acrylic resin.

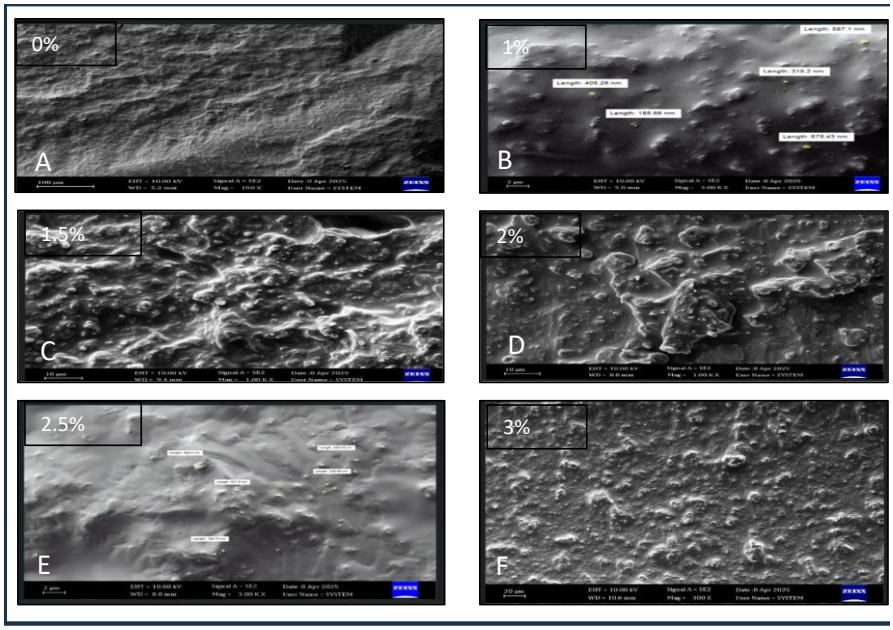

Figure 4: FESEM images of 3D-printed acrylic resin with different BAG concentrations, Surface features vary with increasing nanoparticle content.: (A) 0%, (B) 1%, (C) 1.5%, (D) 2%, (E) 2.5%, (F) 3%.

Table 1**:** Weight percent of bioactive glass nanoparticles combined with 100 cm³ of 3D-printed acrylic resin and the corresponding total mass of added bioactive glass nanoparticles and 3D resin material batch mass.

Group (n = 10)	Nanoparticle Concentration (wt%)	Density 1.2 Weight (gram)	g/cm³ Nano (gram)	Total 3D-resin batch
A (Control)	0%	120	0.0	120
B	1 wt%	120	1.8	118.2
C	1.5 wt%	120	2.7	117.3
D	2 wt%	120	3.6	116.4
E	2.5 wt%	120	4.5	115.5
F	3 wt%	120	5.4	114.6

Table 2: Flexural strength (MPa) mean, standard deviation, minimum, and maximum values.

Groups	Mean ± SD	Minimum	Maximum
A (control)	130.55 ± 2.43	126.0	135.5
B (1%)	131.69 ± 2.19	129.5	135.1
C (1.5%)	135.24 ± 2.25	132.3	139.0
D (2%)	131.06 ± 2.12	128.0	134.2
E (2.5%)	135.22 ± 2.17	132.1	138.9
F (3%)	135.45 ± 2.01	132.7	138.6

Table 3: Mean hardness (Shore D), standard deviation, minimum, and maximum values.

Groups	Mean ± SD	Minimum	Maximum
A (control) [a]	88.18 ± 1.57	85.83	91.17
B (1%)[abc]	88.68 ± 1.44	86.67	90.17
C (1.5%)[b]	89.87 ± 1.20	88.17	91.17
D (2%)[c]	89.93 ± 1.15	89.17	90.83
E (2.5%)[abc]	89.03 ± 0.89	88.00	90.50
F (3%)[abc]	88.85 ± 1.18	86.00	90.33

Note: Different superscript letters indicate statistically significant differences among groups ($p < 0.05$).

Table 4: Surface roughness (µm) mean, standard deviation, minimum, and maximum values.

Groups	Mean ± SD (µm)	Minimum (µm)	Maximum (µm)
A (control)[a]	0.134 ± 0.090	0.063	0.345
B (1%)[b]	0.125 ± 0.101	0.062	0.400
C (1.5%)[abc]	0.102 ± 0.074	0.043	0.297
D (2%)[abc]	0.076 ± 0.034	0.038	0.145
E (2.5%)[abc]	0.097 ± 0.098	0.019	0.368
F (3%)[c]	0.063 ± 0.017	0.044	0.086

Note: Different superscript letters indicate statistically significant differences among groups ($p < 0.05$).

Discussion

Structural characterization

The patterns obtained from XRD confirmed the mainly amorphous structure of BAG and partial crystallization in the composite resin, which can be attributed to reinforcement properties and stability. FTIR-ATR spectra exhibited characteristic bands of both PMMA (C–H, C=O) and BAG (Si–O–Si), with no significant chemical shifts, confirming the physical incorporation and preservation of the silicate framework. Nanoparticle distribution at different concentrations was directly proved with FSEM observations. The specimen in the control group had an even surface. In contrast, BAG-modified specimens were evenly distributed at 1.5-2% and marginally agglomerated at higher loadings.

Currently, there is a notable lack of published research specifically addressing the incorporation of bioactive glass nanoparticles into 3D-printed denture base resins and their influence on physical and mechanical properties. Hence, the interpretation of this study's results largely relies on comparisons with studies that involve conventional heat-polymerized polymethyl methacrylate (PMMA) or silica-based nanoparticles, as most BAG formulations have a high silica composition. Although the differences in the composition and processing technique of resins have been identified, these previous investigations constitute the key to understanding the reinforcement mechanism of nanoparticles in the dental polymer system. In the study, higher loadings (>5%) were avoided to prevent agglomeration, decreased mechanical strength, and poor polymerization, ensuring printability and homogeneous nanoparticle dispersion[2,21].

Flexural strength

Although flexural strength values showed a slight increase with rising BAG concentrations, these differences did not reach statistical significance. This may indicate a potential trend toward improved mechanical performance; however, such interpretation should be considered with caution and cannot be regarded as clinically conclusive without stronger statistical support. This enhancement can be attributed to the quantitative analysis of nanoparticle filler activity, resulting in enhancing the integrity of the polymer matrix by diminishing microdefects and preventing crack formation[27,28].

It has been shown that solid nanoparticles Silicon dioxide and Titanium dioxide improve stress distribution and crack resistance in PMMA when incorporated. The increase is primarily related to their improved percentage, which facilitates activities such as fracture bridging, energy dotting, and robust interfacial bonding with the resin latticework[29]. Nevertheless, excessive filler loading is well-documented to cause matrix saturation, leading to stress concentration zones and a subsequent decline in mechanical performance[30].

Moreover, numerous studies indicate that substantial enhancements in flexural strength generally occur at elevated nanoparticle concentrations, frequently above 5%, when the filler content significantly influences the material's mechanical function[19,20]. Studies on BAG-affected acrylic resins suggest that at high concentrations (e.g., 20%), such products can support flexural strengths above 65 MPa, therefore meeting the ISO 20795 qualification requirements of denture base use[22]. These studies show the potential of BAG as a reinforcing additive for increasing its mechanical properties. The study indicates that the tested concentrations (1–3%) yield a moderate yet continuous improvement in flexural strength, confirming their appropriateness as reinforcement agents in 3D-printed resin systems.

Surface hardness

The addition of BAG resulted in a significant enhancement of surface hardness at concentrations of 1.5% and 2%. The increased performance could have been due to the uniform dispersion of nanoparticles, which may have filled microvoids in the polymer matrix and restricted the mobility of polymer chains, resulting in a denser and more rigid structure[31].

These results align with the most recent studies on silica nanoparticle-reinforced acrylic polymers, which suggest that a broader nanoparticle distribution is associated with improved mechanical performance. The maximum values were observed at 5% loading, and surface hardness continued to improve as silica content increased[32].

Similar trends have been observed in composites that are reinforced with zirconia and aluminum oxide (Al_2O_3) nanoparticles. The surface hardness of PMMA substantially increased at nanoparticle concentrations of 2.5% and 5%, a phenomenon that is linked to the enhancement of interfacial adhesion and the formation of a more compact polymer-filler network[30,33].

These data highlight that nanoparticle composition, concentration, and dispersion quality are key determinants influencing the surface hardness of dental resin composites.

Surface roughness

Denture base materials that produce desirable surface roughness are recommended to make dentures last

longer and inhibit the attachment of microbes on the surface[34]. The increase in BAG was observed to decrease the degree of surface roughness of 3D-printed denture base resin. A 3% concentration was observed to significantly improve the degree of surface roughness compared to 0% and 1% concentrations. The outcomes demonstrate that a greater quantity of BAG nanoparticles might cover the small surface pores and seal the outer surface.

In contrast, an earlier study had suggested that there may be a slight increase in the roughness of conventional acrylic resin surface with high levels of BAG (up to 20%), which could be due to the polymerization technique and leaching out of residual monomer and some soluble particles, leaving void areas responsible for changes in surface roughness[13].

Conversely, a significant reduction of the roughness was noted at the BAG concentration of up to 3%, meaning that the lower concentration ratio is effective in terms of enhancing the surface (by filling the irregularities of the surface) without creating any aggregations and other defects of the surface.

The results confirm the significant effect of both the concentration and distribution of BAG nanoparticles on the final surface characteristics of the resin. Importantly, smoother denture base surfaces are less prone to microbial adhesion and plaque accumulation, which suggests that the reduced roughness achieved with BAG incorporation may contribute to antifouling effects and enhanced long-term clinical performance of dentures.

Although the bioactivity of BAG has been well established in earlier studies, this work did not include direct validation tests such as ion release, pH change, or apatite formation. Similarly, artificial aging protocols (thermocycling, water storage, or mechanical fatigue) were not performed, so the results mainly reflect short-term mechanical behavior. Future study incorporating these methods will help confirm the clinical relevance of BAG-modified 3D-printed denture base resins.

Conclusion

The incorporation of BAG nanoparticles into the 3D-printed denture base resin enhances mechanical and physical characteristics. There was a non-significant progressive increase in flexural strength with rising BAG concentrations. Elevated BAG concentrations, particularly at 1.5% and 2%, markedly improve surface hardness. As the concentration of BAG nanoparticles increased, a gradual reduction in surface roughness was observed, indicating an improvement in surface quality.

References

1. Rezaie F, Dahri M, Farshbaf M, Masjedi M, Maleki R, Amini F. 3D printing of dental prostheses: Current and emerging applications. J Compos Sci. 2023;7(2):80.
2. Ataei K, Ghaffari T, Moslehifard E, Dizaj SM. Physico-chemical and mechanical assessments of a new 3D printed PMMA-based acrylic denture base material. Open Dent J. 2024;18(1):1-6.
3. Karni PA, Maheshwari S, Sarada V, Dass SS, Ananda MN. 3D printing in dentistry: revolutionizing customization and delivery of dental prosthetics. J Neonatal Surg. 2025;14(4):473-8.
4. Dimitrova M, Corsalini M, Kazakova R, Vlahova A, Chuchulska B, Barile G, et al. Comparison between conventional PMMA and 3D printed resins for denture bases: A narrative review. J Compos Sci. 2022;6(3):87.
5. Qadir GO, Abdulkareem JF. An in vitro comparative study of maxillary denture base retention between conventional fabrication and 3D printed techniques. Sulaimani Dent J. 2023;10(2):45-53.
6. Alhotan A, Yates J, Zidan S, Haider J, Silikas N. Flexural strength and hardness of filler-reinforced PMMA targeted for denture base application. Materials (Basel). 2021;14(10):2659.
7. Al-Douri ME, Sadoon MM. Flexural strength, hardness and surface roughness of 3D printed denture base resin reinforced by zinc oxide nanoparticles. J Res Med Dent Sci. 2023;11(1):194-200.
8. Sodagar A, Bahador A, Khalil S, Shahroudi AS, Kassaee MZ. The effect of TiO_2 and SiO_2 nanoparticles on flexural strength of poly (methyl methacrylate) acrylic resins. J Prosthodont Res. 2013;57(1):15-9.
9. Altarazi AT, Jadaan L, McBain AJ, Haider J, Kushnerev E, Yates J. 3D-Printed nanocomposite denture base resin: The effect of incorporating TiO_2 nanoparticles on the growth of Candida albicans. J Prosthet Dent. 2023;130(2):283-9.
10. Altarazi AT, Haider J, Alhotan A, Silikas N, Devlin H. 3D printed denture base material: The

effect of incorporating TiO_2 nanoparticles and artificial ageing on the physical and mechanical properties. J Mech Behav Biomed Mater. 2023;39(10):1122-36.
11. Majeed HF, Hamad TI, Bairam LR. Enhancing 3D-printed denture base resins: A review of material innovations. Sci Prog. 2024;107(3):368504241263484.
12. Aati S, Akram Z, Ngo HC, Fawzy AS. Development of a 3D-printed denture-base resin einforced with silver/zinc oxide mesoporous nanoparticles: mechanical, biological and antibiofilm properties. J Mech Behav Biomed Mater. 2022;134:105418.
13. Alhotan A, Raszewski Z, Chojnacka K, Mikulewicz M, Kulbacka J, Alaqeely R, et al. Evaluating the translucency, surface roughness, and cytotoxicity of a PMMA acrylic denture base reinforced with bioactive glasses. J Funct Biomater. 2024;15(1):16.
14. Jones JR. Review of bioactive glass: From Hench to hybrids. Acta Biomater. 2013;9(1):4457-86.
15. González P, Serra J, Liste S, Chiussi S. Raman spectroscopic study of bioactive silica based glasses. J Non Cryst Solids. 2003;320(1–3):92-9.
16. Misra SK, Mohn D, Brunner TJ, Stark WJ, Philip SE, Roy I. Comparison of nanoscale and microscale bioactive glass on the properties of P(3HB)/Bioglass® composites. Biomaterials. 2008;29(12):1750-61.
17. Liu S, Gong W, Dong Y, Hu Q, Chen X, Gao X. The effect of submicron bioactive glass particles on in vitro osteogenesis. RSC Adv. 2015;5(49):38830-6.
18. Al-Eesaa NA, Johal A, Hill RG, Wong FS. Fluoride-containing bioactive glass composite for orthodontic adhesives: apatite formation properties. Dent Mater. 2018;34(8):1127-33.
19. Raszewski Z, Chojnacka K, Kulbacka J, Mikulewicz M. Mechanical properties and biocompatibility of 3D printing acrylic material with bioactive components. J Funct Biomater. 2023;14(1):13.
20. Raszewski Z, Chojnacka K, Mikulewicz M. Preparation and characterization of acrylic resins with bioactive glasses. Sci Rep. 2022;12(1):16624.
21. Raszewski Z, Nowakowska D, Wieckiewicz W, Nowakowska A. Release and recharge of fluoride ions from acrylic resin modified with bioactive glass. Polymers (Basel). 2021;13(7):1054.
22. Raszewski Z, Chojnacka K, Mikulewicz M, Alhotan A. Bioactive glass-enhanced resins: A new denture base material. Materials (Basel). 2023;16(12):4363.
23. Prpić V, Schauperl Z, Ćatić A, Dulčić N, Čimić S. Comparison of mechanical properties of 3D-printed, CAD/CAM, and conventional denture base resins. J Prosthodont. 2020;29(6):524-8.
24. Raouf L, Faraj S, Azhdar B. Evaluation of flexural strength of heat cure PMMA denture base material reinforced with various concentrations of zirconium oxide. Sulaimani Dent J. 2019;6(2):22-30.
25. Rashid AAL. Some properties of 3D printed acrylic resin material modified by antifungal Vitis vinifera oil. Dent 3000. 2025;1:a001.
26. Gaviria-Martinez A, Castro-Ramirez L, Ladera-Castañeda M, Cervantes-Ganoza L, Cachay-Criado H, Alvino-Vales M, et al. Surface roughness and oxygen inhibited layer control in bulk-fill and conventional nanohybrid resin composites with and without polishing: in vitro study. BMC Oral Health. 2022;22:258.
27. Sasaki Y, Nishizawa Y, Watanabe T, Kureha T, Uenishi K, Nakazono K, et al. Nanoparticle-based tough polymers with crack-propagation resistance. Langmuir. 2023;39(26):9262-72.
28. McCabe JF, Walls AWG. Applied Dental Materials. 9th ed. Chichester (UK): John Wiley and Sons; 2013.
29. Sun L, Gibson RF, Gordaninejad F, Suhr J. Energy absorption capability of nanocomposites: A review. Compos Sci Technol. 2009;69(14):2392-409.
30. Asopa V, Suresh S, Khandelwal M, Sharma A, Saimbi CS, Mathur S. A comparative evaluation of properties of zirconia reinforced high-impact acrylic resin with that of high-impact acrylic resin. J Clin Diagn Res. 2015;9(3):ZC16-9.
31. Rahman MM, Khan KH, Parvez MMH, Irizarry N, Uddin MN. Polymer nanocomposites with optimized nanoparticle dispersion and enhanced functionalities for industrial applications. Processes. 2025;13(4):994.
32. Jayasoman S, Perera DJ, Kodagoda K. Effect of silica nanoparticles on flexural strength and surface hardness of heat polymerized acrylic resin. Bangladesh J Med Sci. 2024;23(10):S79-86.
33. Vojdani M, Bagheri R, Khaledi AAR. Effects of aluminum oxide addition on the flexural strength, surface hardness, and roughness of heat-polymerized acrylic resin. J Dent Sci. 2012;7(3):238-44.
34. Kurzendorfer-Brose L, Rosentritt M. The effect of manufacturing factors on the material properties and adhesion of Candida albicans and Streptococcus mutans on additive denture base material. Materials (Basel). 2025;18(6):1234.

Original Article

Antibacterial and Antibiofilm Activity of *Ziziphora clinopodioides* Essential Oil: An In Vitro Study

Sozyar K. Hakim[*1], *Aram M. Sha*[1]

Abstract

Objective: The present study examined the antibacterial and antibiofilm efficacy of *Ziziphora clinopodioides* (Z. clinopodioides) essential oil (EO) against the primary biofilm colonizers, such as *Streptococcus sanguinis* (S. sanguinis), *Streptococcus mitis* (S. mitis), and *Streptococcus oralis* (S. oralis).

Methods: The hydrodistillation process was used for the essential oil extraction, and its components were analyzed using gas chromatography-mass spectrometry (GC-MS). Antibacterial effect against ATCC strains of S. sanguinis, S. mitis, and S. oralis was assessed using agar well diffusion. Minimal inhibitory concentrations (MICs) and minimal bactericidal concentrations (MBCs) were investigated using the broth macrodilution method. Qualitative tube methods were used to evaluate the antibiofilm efficacy of the Z. clinopodioides EO. 0.12% Chlorhexidine (CHX) served as a positive control.

Results: GC–MS recognized 24 elements with menthol (29.85%), (R)-carvone (10.53%), and eucalyptol (9.88%) as main constituents. Z. clinopodioides EO demonstrated dose-dependent inhibition zones among species and mixtures; generally, inhibition zones were smaller than CHX. The MICs for S. mitis and S. oralis were 2.34 µL/mL, while for S. sanguinis and the three-species mixture were 6.25 µL/mL; The MBCs were 4.68 and 12.5 µL/mL, respectively. The essential oil exhibited weak (S. sanguinis) to moderate (S. mitis, S. oralis, and the mixed culture) antibiofilm activity.

Conclusions: Z. clinopodioides EO demonstrated antibacterial and antibiofilm effectiveness against primary biofilm colonizers; however, its effectiveness was lower than that of chlorhexidine.

Keywords: *Z. clinopodioides EO; Antibacterial efficacy; Antibiofilm activity; Primary biofilm colonizers.*

Submitted: August 27, 2025, Accepted: October 11, 2025, Published: December 1, 2025.

Cite this article as: Hakim SK, Sha AM. Antibacterial and Antibiofilm Activity of Ziziphora clinopodioides Essential Oil: An In Vitro Study. Sulaimani Dent J. 2025;12(3):21-30.

DOI: https://doi.org/10.17656/sdj.10213

1. *Department of Periodontics, College of Dentistry, University of Sulaimani, Sulaimani, Iraq.*

* *Corresponding author*: *sozyar.hakim@univsul.edu.iq.*

Introduction

Periodontitis is an inflammatory disease of microbiological origin in the oral cavity. Dysbiosis between the oral bacteria and host immune response dysregulation enhances the pathogenicity from periodontally healthy states to disease condition[1].

An extensive variety of microorganisms have been found to be pathogenic agents, sometimes called periopathogens[2]. *S. oralis, S. mitis, and S. sanguinis* are considered commensal bacteria that participate in the complex bacterial biofilm formation as primary biofilm colonizers on the tooth surface[3]. Initial colonizers are crucial, creating attachment substrates for later colonizers, including *Porphyromonas gingivalis* and *Fusobacterium nucleatum,* eventually affecting the future phases of biofilm formation and periodontal disease[3-6]. It is advised that, in addition to following good oral hygiene, initiatives are required to limit the development of dental biofilm, periodontal disease, and tooth cavities by targeting the primary colonizers at the first stages of dental biofilm formation[7,8].

Herbal medicines comprise active substances derived from plant parts or other plant parts considered to possess therapeutic properties. Herbal products are favored over traditional pharmaceuticals because of their extensive biological efficacy, enhanced safety characteristics, and reduced expenses. Moreover, conventional medications are recognized for inducing several adverse effects, and prolonged use has led to antibiotic resistance.

Consequently, natural products are being utilized as an alternative for combating or preventing prevalent diseases, including those impacting the oral cavity[9-11].

Ziziphora is a genus within the *Lamiaceae* family, and *Z. clinopodioides* is one of this group's most recognized aromatic and edible species. It is extensively dispersed in Asia and Europe, particularly in Turkey and Iran[12].

In traditional medicine, it has been utilized as a decoction for multiple purposes, including a stomach tonic, sedative, carminative, and antipyretic agent[13]. *Z. clinopodioides* is a potent treatment for many diseases, such as cough, the common cold, bronchitis, headache, viral infections, diarrhea, nausea, typhus, inflammation, edema, cardiovascular disorders, sleeplessness, diabetes, and asthma[14,15]. Additionally, this plant is utilized as a spice to enhance the flavor of food and beverages[15]. Essential oils (EO) consist of volatile compounds derived from aromatic plants. These essential oils have notable biological capabilities, encompassing antibacterial, antifungal, and antioxidant activities[16,17].

Numerous studies have demonstrated the antibacterial activity of *Z. clinopodioides* against *Escherichia coli, Klebsiella pneumoniae, Staphylococcus aureus, Pseudomonas aeruginosa,* and *Salmonella enterica Typhi*[15,18-20]. Furthermore, the antibacterial and antibiofilm properties of *Z. clinopodioides* EO against early biofilm colonizers, such as *S. oralis, S. mitis, and S. sanguinis*, have not been studied before, which is critical during the initial phases of plaque formation. Investigating the efficacy of this botanical compound in inhibiting bacterial proliferation and biofilm development may provide a novel preventive strategy in oral healthcare. This study investigated the antibacterial and antibiofilm properties of *Z. clinopodioides* EO against *S. sanguinis, S. mitis, and S. oralis*. The results may facilitate the creation of diverse plant-derived products to prevent early biofilm formation and reduce the risk of dental biofilm-associated diseases.

Materials and methods

Ziziphora clinopodioides was collected in late Spring from East Kurdistan (Sanandaj governorate). A plant taxonomist from the College of Agriculture at the University of Sulaimani confirmed the identity of plants. The current study was registered and approved by the Ethical Committee of the College of Dentistry at the University of Sulaimani (Approval number 24/252, dated 16 December 2024).

Essential oil extraction

Essential oil (EO) extraction was conducted using hydrodistillation at the Bahar factory in Sulaymaniyah, according to the recognized methodology[21]. Hydrodistillation, using water to extract volatile compounds, is regarded as a gentle technique that reduces the destruction of sensitive ingredients. An appropriate quantity of plant material was positioned in the Novin stainless steel distillation machine (Tehran, Iran), a distillation machine specifically engineered for the factory's requirements. Water was added according to the quantity of the plant, 5 liters for every 1 kilogram of the plant, and upon boiling for 8 hours, the produced steam was passed through the plant. The steam transports the volatile components, and the resulting vapor mixture of steam and oil flows into the condenser, where it is cooled by circulating water, turning the vapor into a liquid mixture of essential oils and water before finally entering the oil separator. Because essential oil has a lower density than water, it separates and floats above the watery layer. The oil was gathered and kept in dark, securely sealed containers at room temperature, resulting in 2–3% essential oils per 100 grams.

GC-MS analysis of the extracted EO

The EO components were recognized using a GC-MS system involving an Agilent (7890A) gas

chromatography-mass spectrometry system (Santa Clara, CA, USA).

Bacterial strains preparation

The bacterial strain was acquired from the American Type Culture Collection (ATCC, Manassas, VA, USA), including reference strains of *S. mitis* (ATCC 49456), *S. oralis* (ATCC 35037), and *S. sanguinis* (ATCC 10556). Following ATCC guidelines, the lyophilized cultures were rehydrated and revived under sterile circumstances.

Thereafter, each strain was cultured in Blood Agar and Brain Heart Infusion (BHI) broth (HiMedia, India). The agar plates and broth were incubated for 24 hours at 37°C in a 5% CO_2 environment generated by a candle inside the jar. The stock cultures were stored in 20% glycerol (Unimedic Pharma, Sweden) at -80 °C for future use (Figure 1).

Essential oil preparation and dissolution

An emulsifying agent was used, which was composed of 10% dimethyl sulfoxide (DMSO) (Merck, Germany) and 0.5% Tween 80 (Biochem-France)[22], due to EO being poorly soluble in water.

Figure 1:(A) *S. sanguinis* (ATCC 10556), (B)*S. mitis* (ATCC 49456), (C) *S. oralis* (ATCC 35037)

Assessment of the minimal inhibitory and minimum bactericidal concentrations

The broth macro dilution method was used to find the MIC of the tested EO[23]. A 400 µL/mL stock solution of *Z. clinopodioides* EO was prepared using 10% DMSO (Merck, Germany) and 0.5% Tween 80 (Biochem, France) as solvents. CHX 0.12% (KIN, SA, Spain) was the positive control, and MHB (HiMedia, India) was the negative control to allow bacterial growth. Two-fold serial dilutions were performed in ten sterile glass test tubes containing 900 µL of Mueller-Hinton broth, supplemented with 100 µL of bacterial inoculum, for MIC detection. Using a loop, a single fresh bacterial colony from a previous 24-hour culture of each species was collected and added to sterile MHB (HiMedia, India) in the tubes. The mixture was then vortexed and standardized to a 0.5 McFarland turbidity standard, equal to 1.5×10^8 CFU/mL. The final volume in each tube was 1 mL, starting with 200 - 0.390 µL/mL for *S. sanguinis* and the three species, and 150 - 0.29 µL/mL for *S. mitis* and *S. oralis*. To more accurately replicate the natural polymicrobial environment, the essential oil MICs were evaluated for each bacterial species individually and in combination. Cotton plugs were used to seal the inoculation tubes, which were then incubated for 24 hours at 37 °C in a candle jar. The MIC was defined as the lowest amount of the essential oil that significantly inhibited the growth of bacteria. After incubation, a series of dilution tubes were checked for bacterial growth, usually as turbidity or a layer of microorganisms at the bottom of the tube. Any tube in the set or dilution series that showed no bacterial growth was the MIC of the essential oils[24].

The MBC was determined by finding concentration that did not allow bacterial growth during the MIC test. A sample was taken from the chosen tubes using a sterile wire loop, placed on agar plates, and kept in a candle jar at 37 °C for 24 hours[25]. It was then determined whether or not bacteria were growing.

Antibiofilm efficacy evaluation

A qualitative tube adhesion approach was used to evaluate the efficacy of the extracts against the biofilms[26]. The inoculated broth used to test the MIC of different EOs was thrown away correctly. To remove planktonic or nonadherent bacteria, the test tubes were washed three times with phosphate-buffered saline (PBS) (Central Drug House, India), pH 7.3. After that, they were turned upside down for 45 minutes to ensure they were completely dry. Next, each tube was given 1 mL of 1% crystal violet and left at room temperature for 15 minutes. Rinsing the tubes three times with sterile distilled water eliminated the rest of the dye. The biofilm formation was evaluated qualitatively by observing (examiner's vision) the violet color on the wall and bottom of the tubes, then classifying it based on the intensity of the violet color as nonadherent (0), weakly adherent (+), moderately adherent (++), or firmly adherent (+++)[27]. All tests were done three times. The same protocols for antibiofilm activity were used with three different species at the same time.

Statistical analysis

The results are shown as mean ± standard deviation and were analyzed using SPSS software version 27 (SPSS Inc., Chicago, IL, USA). The independent t-test was employed for comparisons, with $p \leq 0.05$ indicating statistical significance.

Results

Ordering specific bacterial strains

Colonies of *S. sanguinis* are usually small and can be grayish or colorless; however, *S. mitis* and *S. oralis* are classified as alpha-hemolytic *streptococci*, signifying that they generate a greenish color around the colonies on blood agar (Figure 1).

GC-MS Examination of Bioactive Compounds

GC-MS analysis of *Z. clinopodioides* EO

The GC-MS analysis of the *Z. clinopodioides* EO identified 24 compounds. The main compound was menthol (29.85%), (R)-Carvone (10.533%), Eucalyptol (9.883%), L-β-pinene (6.278%), and p-Menthan-3-one (5.259%), as shown in Table 1.

Antibacterial Activity

The Antibacterial Efficacy of *Z. clinopodioides* EO

As shown in Table 2 and Figure 2, the essential oil of *Z. clinopodioides* exhibited concentration-dependent effects, characterized by an increase in inhibition zones corresponding to rising EO concentrations. It worked against *S. mitis* and *S. oralis* at 30%, 40%, and 50% concentrations, against *S. sanguinis* and all three species together at 40% and 50% concentrations. The inhibition zones for *S. mitis* were between 9.55 ± 1.0 mm and 17.99 ± 1.0 mm, and for *S. oralis*, they were between 7.0 ± 1.0 mm and 8.32 ± 0.3 mm. At 30% EO, *S. sanguinis,* and three species together showed no inhibition, but they did show zones of 8.92 ± 0.8 mm and 9.88 ± 0.5 mm at 40% and 50%, respectively, 7.8 ± 0.4 mm at 40% and 8.92 ± 1.5 mm at 50% against three species together. The agar well diffusion assay controls, which had 10% dimethyl sulfoxide and 0.05% Tween-80, did not have an inhibition zone. CHX, on the other hand, had much

bigger inhibition zones: 21.51 ± 1.0 mm for *S. mitis*, 18.89 ± 0.9 mm for *S. sanguinis*, 19.61 ± 0.6 mm for *S. oralis*, and 16.38 ± 1.4 mm for the three species together. CHX generally had a larger inhibition zone than the tested EO, as shown in Table 2.

MIC and MBC evaluation of *Z. clinopodioides* EO against the bacterial strain

The broth macro dilution method was used for the evaluation of the MICs of *Z. clinopodioides* EO against bacterial strains, which were 2.34 µL/mL for *S. oralis* and *S. mitis*, but 6.25 µL/mL for *S. sanguinis* and the three species together. The MBCs, illustrated in Figure 3, were 4.68 µL/mL for *S. oralis* and *S. mitis*; however, 12.5 µL/mL for *S. sanguinis* and the three species, as shown in Table 3.

Antibiofilm properties of *Z. clinopodioides* EO

The tube assay results showed that *Z. clinopodioides* EO affected how bacteria stuck to surfaces and formed biofilms. The amount of violet crystal deposition on the inner tube surfaces was used to measure biofilm formation. Darker staining meant that there was more biofilm present. The oil significantly affected biofilm production, even at the lowest concentration tested. The oil decreased biofilm adherence at its MIC, showing weak activity against *S. sanguinis* and moderate inhibitory effects on *S. mitis, S. oralis*, and the three species. In contrast, 0.12% CHX completely stopped biofilm growth for *S. sanguinis* and *S. oralis*. The negative control tubes, which only had bacterial inoculum in MHB, showed a lot of biofilm buildup, as shown in Table 4 and Figure 3.

Table 1: Results of GC-MS analysis of Z. clinopodioides EO.

Peak	R. T	Area%	MW	MF	CAS#	Compound name
1	4.16	1.643	100	C6H12O	928-96-1	3-Hexen-1-ol, (Z)-
2	4.395	1.254	136	C10H16	7785-70-8	1R-α-Pinene
3	5.423	6.278	136	C10H16	18172-67-3	L-β-pinene
4	6.217	0.045	136	C10H16	99-86-5	1,3-Cyclohexadiene, 1-methyl-4-(1-methylethyl)-
5	6.289	0.191	130	C8H18O	589-98-0	3-Octanol
6	6.434	1.882	136	C10H16	5989-27-5	D-Limonene
7	6.827	9.883	154	C10H18O	470-82-6	Eucalyptol
8	7.08	0.319	136	C10H16	99-85-4	γ-Terpinene
9	7.55	0.015	136	C10H16	586-62-9	Terpinolen
10	8.034	0.402	154	C10H18O	78-70-6	Linalool
11	9.033	0.232	154	C10H18O	89-79-2	L-isopulegol
12	9.208	1.006	156	C10H20O	491-01-0	Neomenthol
13	9.361	5.259	154	C10H18O	10458-14-7	p-Menthan-3-one
14	9.584	29.85	156	C10H20O	2216-51-5	Menthol
15	10.373	0.083	170	C10H18O2	53404-49-2	Bicyclo(3.1.1)heptane-2,3-diol, 2,6,6-trimethyl
16	10.956	2.161	198	C12H22O2	20777-45-1	Isomenthol acetate
17	11.222	10.533	150	C10H14O	6485-40-1	(-)-(R)-Carvone
18	11.782	1.719	150	C10H14O	499-75-2	Carvacrol
19	13.852	0.057	204	C15H24	483-76-1	δ-Cadinene
20	13.943	0.083	154	C10H18O	562-74-3	4-Terpinenol
21	14.078	0.126	154	C10H18O	10482-56-1	α-Terpineol
22	15.164	0.287	222	C15H26O	511-67-1	Epiglobulol
23	15.885	0.075	220	C15H24O	1139-30-6	Caryophyllene oxide
24	16.126	0.054	220	C15H24O	1139-30-6	β-Caryophyllene oxide

Area%: Compound percentage; CAS#: Registry number; MW: Molecular weight (g/mol); MF: Molecular formula, R. T: Retention time

Table 2: Mean and standard deviations of inhibition zones and p-values of CHX and *Z. clinopodioides* EO at different concentrations against S. mitis, S. sanguinis, S. oralis, and the three species together.

Oil%	Inhibition zone (*S. mitis*)			Inhibition zone (*S. sanguinis*)		
	***Z. clinopodioides*EO**	**CHX0.12%**	***p*-value**	***Z. clinopodioides*EO**	**CHX0.12 %**	**p-value**
30%	9.55±1.0	21.77±1.0	0.00			
40%	13.77±3.3	21.0±1.0	0.02	8.92±0.8	18.24±0.2	0.00
50%	17.99±1.7	21.77±1.0	0.03	9.88±0.5	19.55±1.6	0.001
	Inhibition zone (*S. oralis*)			Inhibition zone (three species)		
30%	7.0±1.0	20.33±0.8	0.00			
40%	7.99±1.3	18.51±0.4	0.00	7.8±0.4	16.44±1.3	0.00
50%	8.32±0.3	19.99±0.6	0.00	8.92±1.5	16.33±1.5	0.004

The t-test was used for comparisons, and $p \leq 0.05$ was considered statistically significant.

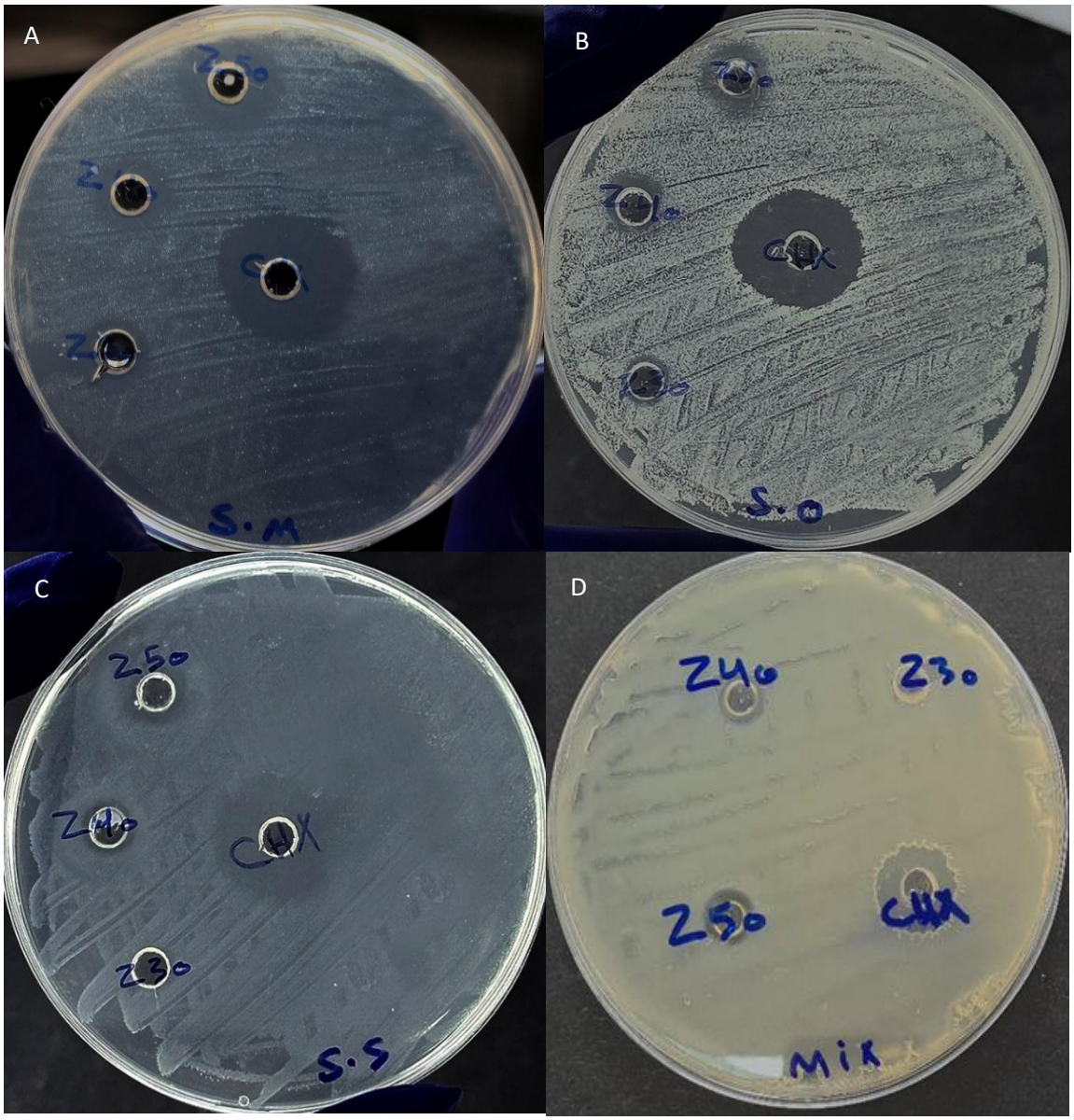

Figure 2: Antibacterial susceptibility with different concentrations (30%, 40% and 50%) for *Z. clinopodioides* EO by agar well diffusion method against (A) *S.mitis*, (B) *S. oralis*, (C) *S.sanguinis*, and (D) the three species together. Z30: *Z. clinopodioides* 30%, Z40: *Z. clinopodioides* 40%, Z50: *Z. clinopodioides* 50%, CHX: Chlorohexidine 0.12%

Table 3: The MIC and MBC values of *Z. clinopodioides* EO on bacterial strains.

Bacteria	*Z. clinopodioides* EO	
	MIC	MBC
S. oralis	2.34 µL/mL	4.68 µL/mL
S. sanguinis	6.25µL/mL	12.5µL/mL
S. mitis	2.34µL/mL	4.68µL/mL
Three species together	6.25µL/mL	12.5µL/mL

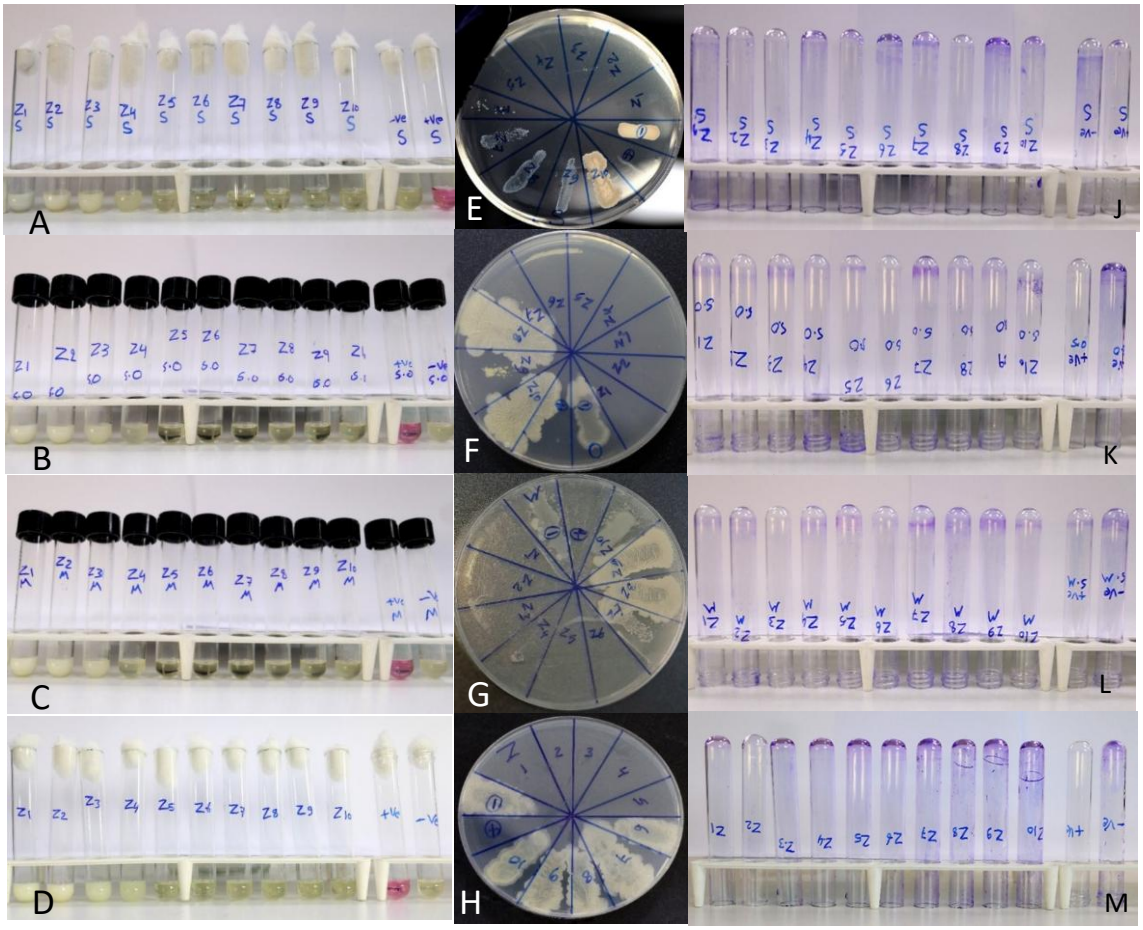

Figure 3*:* A, B, C, and D: Broth macro dilution method to determine MIC values, E, F, G, and H: Agar culture method to confirm MBCs and I, J, K, L: Qualitative antibiofilm assay using the tube method to assess the anti-biofilm activity of a two-fold dilution series of *Z. clinopodioides* EO on *S. sanguinis, S. oralis, S. mitis,* and the three species together, respectively.

Table 4: Qualitative biofilm formation of the *Z. clinopodioides* EO.

Bacteria	Z. clinopodioidesEO	CHX (positive control)	MHB (negative control)
S. oralis	++	0	+++
S. sanguinis	+	0	+++
S. mitis	++	+	+++
Three species together	++	0	+++

Discussion

Periodontitis is a complicated inflammatory disease with multiple contributing factors. One of the most critical factors that affects the development and progression of periodontal disease is an increase in the number of pathogenic bacteria in dental biofilm, which triggers a massive immune response[28]. The current study displays that Ziziphora EO prevents growth and lessens biofilm development of primary colonizers such as *S. sanguinis, S. mitis*, and *S. oralis*. These strains are the essentials and form the base for the attachment of secondary colonizers, "red-complex" bacteria, linking initial colonization to periodontal disease progression[1,4]. Natural EOs could contribute to biofilm control within preventive approaches by targeting these initial colonizers.

Using this natural product as a preventive or therapeutic agent is a good alternative to chemical and traditional antibacterial agents that have many adverse effects, such as tooth discoloration, taste alterations, burning sensations, and the emergence of bacterial resistance[29,30]. This *in vitro* study evaluated the antibacterial and antibiofilm effectiveness of *Z. clinopodioides* EO against primary biofilm colonizers, specifically *S. oralis, S. mitis,* and *S. sanguinis*, obtained from ATCC. The GC-MS analysis was used to determine the main compounds of the *Z. clinopodioides* EO, namely menthol (29.85%), (R)-Carvone (10.533%), Eucalyptol (9.883%), which enhance the *Z. clinopodioides* EO bioactivity as antibacterial and antibiofilm agent. Lamiaceae species are recognized for membrane-active monoterpenes that escalate cell-membrane permeability and can harm exopolysaccharide production and bacterial quorum sensing[16,17]. The detected growth inhibition zones and qualitative antibiofilm are consistent with such properties.

The findings demonstrated that *Z. clinopodioides* EO exhibits antibacterial efficacy against bacterial strains, as assessed by agar well diffusion and broth macro dilution techniques, with a significant difference in the average diameter of the inhibitory zone at various doses of *Z. clinopodioides* EO. Therefore, it may be stated that clarifying the impact of the oil increases with higher concentration. The comparison of the inhibition zone of *Z.clinopodioides* EO with that of a positive control group revealed that bacterial growth in the presence of chlorhexidine (CHX) was lower than that of *Z. clinopodioides* EO at concentrations of 30%, 40%, and 50%, for *S. oralis,* and *S. mitis,* 40%, and 50%, for *S. sanguinis,* and three species together. Moreover, the *Z. clinopodioides* EO exhibited diminished efficacy against the three bacterial strains collectively, when bacteria grow together, forming a polymicrobial, more complex, and more protective biofilm that may minimize the antibacterial effect of the EO[31].

In the present study, the EO demonstrated bacteriostasis/bactericidal effects, with mean MICs of 2.34 µL/mL for *S. oralis and S. mitis*, and 6.25µL/mL for *S. sanguinis, and* the polymicrobial mixture, MBCs were 4.68 and 12.5 µL/mL, respectively. The three-species mixture and S. sanguinis's higher MIC/MBC compared to the other two strains are due to intrinsic differences in the sensitivity and protective influence of the polymicrobial community. Antimicrobial tolerance in mixed communities can be enhanced by metabolic cooperation, physical shielding, and changed gene expression[31]. These results highlight the necessity of testing potential treatments in multispecies models that more closely resemble clinical plaque in addition to single strains. Other investigators reported a MIC against other non-oral pathogens that was equivalent to 3 µg/mL, 67 µg/mL, 33 µg/mL, 33 µg/mL, and 67 µg/mL for *Escherichia coli, Klebsiella pneumoniae, Staphylococcus aureus, Pseudomonas aeruginosa,* and *Salmonella enterica Typhi*, respectively[18]. However, no previous studies on periodontal pathogens were available to compare with the current findings.

The discrepancies in MIC values documented by various studies across regions are primarily linked to the chemical composition and concentration of active constituents in essential oils, which are substantially affected by plant genotype and environmental factors, including geographical conditions, soil properties, temperature, harvesting season, and, importantly, the oil extraction technique. Additionally, other factors may influence the MIC values, including variations in antibacterial testing methodologies, such as the formulation of the growth medium, incubation parameters, and the emulsifying agents or solvents utilized, which may modify the bactericidal efficacy of the essential oils. Furthermore, variations in the cell wall architecture across various strains of the same bacterial species may also affect MIC outcomes[32].Moreover, *Z. clinopodioides* EO demonstrated antibiofilm efficacy against bacterial strains, as assessed by the qualitative tube method. Methods interrupting any stage of biofilm formation may be beneficial in treating biofilm-related periodontal diseases[33].

The analysis of the results showed that *Z. clinopodioides* EO had a weak antibiofilm effect against *S. sanguinis*; however, it had a moderate antibiofilm effect against *S. mitis, S. oralis,* and the three species together. Several studies reported the antibiofilm potential of *Z. clinopodioides* EO[34,35]; however, no previous investigation has demonstrated the antibiofilm activity of the *Z. clinopodioides* EO on periodontal pathogens.

The present study offers significant findings into the antibacterial and antibiofilm effectiveness of *Z. clinopodioides* EO against primary biofilm colonizers using ATCC bacterial strains. As anticipated, 0.12% of CHX inhibited biofilm formation totally and performed better than EO. The gold standard CHX remains the clinical standard[10]. Concerns regarding ecological effects on the microbiome, tooth discoloration, taste disruption, and mucosal irritation may limit the long-term use of CHX. For these reasons, there is interest in botanical adjuncts that may enable dose-sparing or intermittent use.

However, certain limitations should be acknowledged. Standard laboratory strains may not represent the phenotypic diversity, resistance mechanisms, or biofilm-forming abilities of clinical or environmental isolates. Furthermore, the *in vitro* experimental framework does not replicate the intricate biological environments found *in vivo*, where aspects such as host immune responses, nutritional gradients, and surface properties can significantly influence biofilm formation and antimicrobial efficacy. Further research is required regarding the activity of the *Z. clinopodioides* EO against other oral bacteria, especially periodontal pathogens, and additional investigation about the active compounds of *Z. clinopodioides* extracts in different places and seasons.

Conclusion

Z. clinopodioides EO, abundant in menthol, (R)-Carvone, and other monoterpenes, demonstrated antibacterial and antibiofilm effectiveness against key primary colonizers such as *S. sanguinis, S. oralis, and S. mitis*. However, it was still less effective than chlorhexidine.

References

1. Hajishengallis G, Lamont RJ. Beyond the red complex and into more complexity: the polymicrobial synergy and dysbiosis (PSD) model of periodontal disease etiology. Mol Oral Microbiol. 2012;27(6):409-19.
2. Golub LM, Lee HM. Periodontal therapeutics: current host-modulation agents and future directions. Periodontol 2000. 2020;82(1):186-204.
3. Kreth J, Merritt J, Qi F. Bacterial and host interactions of oral streptococci. DNA Cell Biol. 2009;28(8):397-403.
4. Diaz PI, Chalmers NI, Rickard AH, Kong C, Milburn CL, Palmer RJ, et al. Molecular characterization of subject-specific oral microflora during initial colonization of enamel. Appl Environ Microbiol. 2006;72(4):2837-48.
5. Engel AS, Kranz HT, Schneider M, Tietze JP, Piwowarcyk A, Kuzius T, et al. Biofilm formation on different dental restorative materials in the oral cavity. BMC Oral Health. 2020;20(1):162.
6. Li J, Helmerhorst EJ, Leone CW, Troxler RF, Yaskell T, Haffajee AD, et al. Identification of early microbial colonizers in human dental biofilm. J Appl Microbiol. 2004;97(6):1311-8.
7. Marsh PD. Dental plaque as a biofilm and a microbial community–implications for health and disease. BMC Oral health. 2006;6(Suppl 1):S14.
8. Marsh PD. Microbial ecology of dental plaque and its significance in health and disease. Adv Dent Res. 1994;8(2):263-71.
9. Eid Abdelmagyd HA, Ram Shetty DS, Musa Musleh Al-Ahmari DM. Herbal medicine as adjunct in periodontal therapies- A review of clinical trials in past decade. J Oral Biol Craniofac Res. 2019;9(3):212-217.
10. James P, Worthington HV, Parnell C, Harding M, Lamont T, Cheung A, et al. Chlorhexidine mouthrinse as an adjunctive treatment for gingival health. Cochrane Database Syst Rev. 2017;3(3):CD008676.
11. Sha AM, Garib BT. Antibacterial Effect of Curcumin against Clinically Isolated Porphyromonas gingivalis and Connective Tissue Reactions to Curcumin Gel in the Subcutaneous Tissue of Rats. BioMed Res Int. 2019;2019(1):6810936.
12. Shahbazi Y. Ziziphora clinopodioides Essential Oil and Nisin as Potential Antimicrobial Agents against Escherichia coli O157:H7 in Doogh (Iranian Yoghurt Drink). J Pathog. 2015;2015:176024.
13. Salehi P, Sonboli A, Eftekhar F, Nejad-Ebrahimi S, Yousefzadi M. Essential Oil Composition, Antibacterial and Antioxidant Activity of the Oil and Various Extracts of Ziziphora clinopodioides subsp. rigida (BOISS.) RECH. f. from Iran. Biol Pharm Bull. 2005;28(10):1892-6.
14. Ahmadi A, Gandomi H, Derakhshandeh A, Misaghi A, Noori N. Phytochemical composition and *in vitro* safety evaluation of *Ziziphora clinopodioides* Lam. ethanolic

extract: Cytotoxicity, genotoxicity and mutagenicity assessment. J Ethnopharmacol. 2021;266:113428.
15. Sonboli A, Mirjalili MH, Hadian J, Ebrahimi SN, Yousefzadi M. Antibacterial activity and composition of the essential oil of Ziziphora clinopodioides subsp. bungeana (Juz.) Rech. f. from Iran. Z Naturforsch C J Biosci. 2006 Sep;61(9-10):677-80.
16. Khorshidian N, Yousefi M, Khanniri E, Mortazavian AM. Potential application of essential oils as antimicrobial preservatives in cheese. Innov Food Sci Emerg Technol. 2018;45:62-72.
17. Sharma S, Barkauskaite S, Jaiswal AK, Jaiswal S. Essential oils as additives in active food packaging. Food Chem. 2021;343:128403.
18. Shahbazi Y. Chemical Composition and in Vitro Antibacterial Effect of Ziziphora clinopodioides Essential Oil. Pharm Sci. 2015;21(2):51-6.
19. Behravan J, Ramezani M, Hassanzadeh MK, Eskandari M, Kasaian J, Sabeti Z. Composition, Antimycotic and Antibacterial Activity of Ziziphora clinopodioides Lam. Essential Oil from Iran. J Essent Oil Bear Plants. 2007;10(4):339-45.
20. Shahbazi Y, Shavisi N. Interactions of *Ziziphora clinopodioides* and *Mentha spicata* essential oils with chitosan and ciprofloxacin against common food-related pathogens. LWT - Food Sci Technol. 2016;71:364-9.
21. Tongnuanchan P, Benjakul S. Essential oils: extraction, bioactivities, and their uses for food preservation. J Food Sci. 2014;79(7):R1231-49.
22. Rasheed AH, Gul SS, Azeez HA. Antibacterial and antibiofilm profiles of Thymus Vulgaris essential oil on clinically isolated Porphyromonas Gingivalis and Prevotella Intermedia: an in vitro study. Sulaimani Dent J. 2022;9(2):53-63.
23. Balouiri M, Sadiki M, Ibnsouda SK. Methods for in vitro evaluating antimicrobial activity: A review. J Pharm Anal. 2016;6(2):71-9.
24. Rao J, Chen B, McClements DJ. Improving the Efficacy of Essential Oils as Antimicrobials in Foods: Mechanisms of Action. Annu Rev Food Sci Technol. 2019;10(1):365-87.
25. Pellegrini M, Ricci A, Serio A, Chaves-López C, Mazzarrino G, D'Amato S, et al. Characterization of essential oils obtained from Abruzzo Autochthonous plants: antioxidant and antimicrobial activities assessment for food application. Foods. 2018;7(2):19.
26. Hukić M, Seljmo D, Ramovic A, Ibrišimović MA, Dogan S, Hukic J, et al. The effect of lysozyme on reducing biofilms by Staphylococcus aureus, Pseudomonas aeruginosa, and Gardnerella vaginalis: an in vitro examination. Microb Drug Resist Larchmt N. 2018;24(4):353-8.
27. Eladawy M, El-Mowafy M, El-Sokkary MMA, Barwa R. Effects of lysozyme, proteinase k, and cephalosporins on biofilm formation by clinical isolates of Pseudomonas aeruginosa. Interdiscip Perspect Infect Dis. 2020;2020(1):6156720.
28. Liccardo D, Cannavo A, Spagnuolo G, Ferrara N, Cittadini A, Rengo C, et al. Periodontal disease: a risk factor for diabetes and cardiovascular disease. Int J Mol Sci. 2019;20(6):1414.
29. Petrovski M, Terzieva-Petrovska O, Taskov T, Papakoca K. Side effects associated with chlorhexidine mouthwashes use. Maced Pharm Bull. 2022;68(sup 1):377-8.
30. Scribante A, Gallo S, Pascadopoli M, Frani M, Butera A. Ozonized gels vs chlorhexidine in non-surgical periodontal treatment: A randomized clinical trial. Oral Dis. 2024;30(6):3993-4000.
31. Hibbing ME, Fuqua C, Parsek MR, Peterson SB. Bacterial competition: surviving and thriving in the microbial jungle. Nat Rev Microbiol. 2010;8(1):15-25.
32. Van de Vel E, Sampers I, Raes K. A review on influencing factors on the minimum inhibitory concentration of essential oils. Crit Rev Food Sci Nutr. 2019;59(3):357-78.
33. Chapple ILC, Mealey BL, Van Dyke TE, Bartold PM, Dommisch H, Eickholz P, et al. Periodontal health and gingival diseases and conditions on an intact and a reduced periodontium: Consensus report of workgroup 1 of the 2017 World Workshop on the Classification of Periodontal and Peri-Implant Diseases and Conditions. J Periodontol. 2018;89 Suppl 1:S74-84.
34. Hamidi M, Toosi AM, Javadi B, Asili J, Soheili V, Shakeri A. In vitro antimicrobial and antibiofilm screening of eighteen Iranian medicinal plants. BMC Complement Med Ther. 2024;24(1):135.
35. Shahbazi Y. Antibacterial effects of Ziziphora clinopodioides and Mentha spicata essential oils against common food-borne pathogen biofilms on stainless steel surface. Bulgarian Journal of Veterinary Medicine. 2020;23(1):29.

Original Article

The Effects of Different Attachment Geometries on Second Molar Uprighting in Clear Aligner Treatment: An In Vitro Study

Hawre M. Maarouf [*1], *Trefa M. Ali Mahmood* [1]

Abstract

Objective: Investigate the biomechanical impacts of various attachment designs on second molar uprighting, identify optimal geometry, and provide clinical guidelines for clear aligner treatment following first molar loss.

Methods: This in vitro study was conducted by using 3D-printed dental models with mesially tilted second molars. Five groups were designed based on attachment geometry: one without attachment, horizontal, inclined attachment, twin alternative, and two vertical. Clear aligners were fabricated and applied to each model to deliver uprighting forces. Pre- and post-treatment tooth positions were measured to a fixed reference point by using CBCT, and changes in mesiodistal inclination, buccolingual inclination, vertical, and mesiodistal distances were recorded. Statistical analysis was performed using the Kruskal-Wallis test followed by pairwise comparisons to identify significant differences among groups.

Results: The inclined attachment produced the greatest uprighting effect in mesiodistal inclination, indicating superior molar control compared to other geometries. Minimal buccolingual inclination change was observed in the single horizontal and inclined groups, while twin-type attachments showed greater deviation. Vertical positioning was largely maintained across groups, with no statistically significant differences. Mesiodistal distance varied between attachment types, with inclined and horizontal designs showing the greatest reduction. Overall, attachment geometry demonstrated measurable effects on molar movement across multiple dimensions.

Conclusions: The inclined attachment showed better performance in second molar uprighting compared with single horizontal, twin, and two vertical attachments. Attachment geometry significantly influences molar control.

Keywords: *Clear Aligner; Attachment Geometry; Orthodontic Tooth Movement and Biomechanics.*

Submitted: August 7, 2025, Accepted: October 21, 2025, Published: December 1, 2025.

Cite this article as: Maarouf HM, Mahmood TM. The Effects of Different Attachment Geometries on Second Molar Uprighting in Clear Aligner Treatment: An In Vitro Study. Sulaimani Dent J. 2025;12(3):31-41.

DOI: https://doi.org/10.17656/sdj.10214

1. *Department of Orthodontics, College of Dentistry, University of Sulaimani, Sulaimani, Iraq.*

** Corresponding author*: *hawre.maarouf@univsul.edu.iq.*

Introduction

Clear Aligner Treatment (CAT) is a method for straightening the teeth by using transparent, custom-made plastic aligners. The aligners move the teeth into the intended position by gradually exerting gentle force[1]. Among the benefits of CAT are virtually invisible braces that are comfortable to wear and detachable for brushing and eating, and this results in more hygienic treatment as compared to fixed orthodontics. This allows CAT to be utilized in treating a vast array of orthodontic issues[2].

The first permanent molars are highly prone to dental caries, which often results in their premature loss. The early loss of first molars in isolation is a prevalent issue globally, affecting from 8% to 21% of the population, with this variation reflecting differences in the age groups, populations studied, and other methodological variables[3]. This occurrence is likely due to these teeth being the first to emerge in the posterior of the mouth and can be attributed to enamel developmental issues such as molar incisor hypomineralization. The prevalence of this condition ranges from 2.4% to 40.2%[4,5]. As a result of this extraction, the second molar will tip to the extraction space. This condition is frequently observed in adults who are seeking orthodontic treatment and is linked to occlusal interference, periodontal issues, and difficulties in rehabilitating the edentulous area[6]. This tilting happens because of the loss of mesial support of the tooth, and it drifts forward under occlusal and eruptive forces, as the crown moves mesially and the root remains in distal. The degree of tipping may differ between patients depending on factors such as the timing of molar loss relative to second-molar eruption, the amount of available space, and the magnitude of functional and occlusal forces[7]. Furthermore, with the introduction of high-tech appliances, anchorage devices, and improved patient awareness of the risks associated with maxillofacial surgery, treating complex situations with orthodontic treatment has become more difficult in recent years[8].

Some drawbacks to conventional fixed orthodontic treatment for molar uprighting include the tilted molar's extrusion, unintended reciprocal movement of the anchorage units, the requirement for large appliances, and lengthier treatment times[9]. Another drawback of fixed orthodontic treatment is the development of white spot lesions around orthodontic attachments. In contrast, removable appliances such as clear thermoplastic aligners are easily removed, allowing patients to practice oral hygiene comfortably. Since patients do not experience any obstructions from brackets, bands, or arch wires, they may prevent their oral hygiene from deteriorating[10].

Some aligner systems use resin-bonded attachments. Attachments have been used to make sure that the appliance remains steady in its place on the teeth and to enhance CA's capability to perform certain movements that would otherwise be impossible. Unpredictable movements consist of rotation of round-shaped teeth (from an occlusal perspective), extrusion of teeth, and retention of aligners in those cases where teeth are short or do not have enough undercut. Only minimal tooth movement can be obtained when bonded attachments are absent from an aligner system[11].

Clear aligners are indicated to correct inclinations of the teeth to their normal position, movement that is considered difficult unless the correct attachment is used. Recent studies have focused on anterior teeth, and suitable attachment for correcting tilted second molars is controversial[12]. A limited number of researchers have explored the possibility of molar uprighting with clear aligners. For example, a recent case report described uprighting and protraction of a mandibular second molar using a dual approach that integrated aligners with an auxiliary cantilever arm, resulting in successful crown and root movement with high accuracy[13].

Systematic reviews highlight that attachments improve the effectiveness of aligners for specific movements, like mesiodistal tipping, root torque, and intrusion but their specific role in posterior uprighting has not been conclusively validated, showing the need for further investigation[11]. The objective of this study is to find the most suitable and efficient attachment geometries to correct this malocclusion with clear aligners.

Materials and methods

Preparing the typodont for this study began with the digital scanning of a standard typodont using the Shining 3D® Aoralscan 3™ intraoral scanner. This scanner, operated through the DentalOrder software, produced a high-quality OBJ file representing the initial morphology of the standard typodont model. (Figure 1:A). The scan was subsequently transferred into the MEDIT™ software version 3.0 (Medit Corp., Seoul, South Korea) to generate a digital working cast. In this digital working cast, the lower left molar region was eliminated. (Figure 1:B)

The digital working cast was then imported into Blender™ software version 3.6 LTS (Blender Foundation, Amsterdam, Netherlands), a 3D modeling software, to further prepare it for experimental use. In Blender, a supporting box structure was placed in the area of the missing molars, with dimensions sufficient to stabilize the addition of future components; the dimensions were w:14 mm, L:30 mm and H:19 mm[12].

Nine small wells of 2 mm × 2 mm × 2 mm were designed within the large box wall, four of them in the sagittal plane and four in the coronal plane, and one at the

intersection of the two planes. (Figure 1:C). The aim of these cubes was to serve as radiographic reference markers during the study. This arrangement is necessary for comparing data from before and after the experiment in a scientific way. Following finalization of the digital design, the model was printed using a high-precision Microlay 3D printer with layer thicknesses of 100 microns using KeyModel Ultra™ dental model resin (Keystone Industries, USA). (Figure 1:D)

The first physical printed model was then used to make the typodonts. The spaces of the nine small cubes were filled with flowable composite— Esflow® (Spident Co., Ltd., Incheon, South Korea). Composite placement was done carefully to avoid gaps, and polymerization was performed using a Wiscure-1S+™ (Wismed, China) light-curing unit, ensuring the reference points remained fixed and visible under CBCT imaging. (Figure 2:A). Then typodont wax was used to fill the supporting box, serving as a base for seating a mandibular second molar tooth. After that, aluminum-based tooth was used in the study because this material has the ability to minimize scattering artifacts during CBCT imaging[15]. The tooth was manually positioned within the wax at an angle of 30 degrees to the horizontal reference plane, representing a typical malposition often encountered in clinical orthodontics in cases with early extraction of the permanent lower first molar[16]. (Figure 2:B)

Taking initial records

A Cone Beam Computed Tomography (CBCT) scan was taken to serve as the initial reference for evaluating the spatial relationship between the tilted mandibular second molar and the composite-filled reference cubes. The imaging was taken by using the VATECH® Pax-i3D™ CBCT (VATECH Co., Ltd., Korea) unit, operated through its default software, Ez3D-I™ (VATECH Co., Ltd., Korea), which manages image acquisition and reconstruction. The field of view of this machine is 100 mm in diameter and 85 mm in height, and the exposure parameters were 94 kVp and 7.4mA. Low-dose mode was selected with a voxel size of 0.2 mm, which gave enough spatial resolution for our study. The DICOM data obtained from this exposure was used to assess the spatial position of the molar with the fixed coordinates of the reference cubes in terms of mesiodistal inclination, buccolingual inclination, and mesiodistal and apicogingival. The furcation point and the long axis of the tooth were used to make these calculations. (Figure 3)

Duplication of the typodont

After carefully inspecting the CBCT of the first typodont and confirming that the tooth lay on the same plane as the reference point, we started the process of making a new typodont. A new scan of the first typodont was obtained using the same scanner that was mentioned earlier. Using this scan, a rigid guide was created to precisely place the tooth in the same spatial location in the new typodonts. Additionally, the clear aligners were made using this same scan. (Figure 4:A)

The OBJ file was imported into the RealGUIDE™ software version 5.4 (3DIEMME S.r.l., Italy) program, where two guides were designed with different paths of insertion: one from the mesio-buccal direction and the other from the disto-lingual direction. This two-guide method makes sure that the teeth are in the right place with great accuracy and stability. (Figure 4:B)

The STL files of the guides were imported and printed using the MicroForm™ software (Microlay S.L., Spain) with Dentona® Surgical Guide Resin (Dentona GmbH, Dortmund, Germany) on the Microlay® Versus 365™ printer (Microlay S.L., Spain), configured at a 100-micron layer thickness[17]. (Figure 4:C)

After printing, the guides were washed in 96% ethanol for 3 minutes for two cycles using the Anycubic™ wash and cure (Anycubic Technology Co., Ltd., Shenzhen, China) to remove excess resin. They were then post-cured in the same machine for 10 minutes to ensure complete polymerization and eliminate any residual monomers. Using the KeyModel resin and Microlay printer, 14 additional typodonts were printed. With the aid of the surgical guide, the tooth was accurately positioned in each new typodont, replicating the spatial position of the tooth in the original model. New CBCT scans had been taken of the new typodont to make sure that the teeth were in the same place as they were in the original one. (Figure 4:D)

Making Clear Aligners

The same scan used for surgical guide fabrication was imported into Maestro 3D™ software version 5.1 (AGE Solutions, Italy) to design a series of clear aligners incorporating various attachment geometries. During the base detection process, the supporting box was removed to facilitate the thermoforming process. This adjustment was necessary to eliminate a large undercut adjacent to the tooth, which could adversely affect the adaptation and fit of the thermoformed aligner sheets.

In the virtual setup, the mandibular second molar was initially inclined at 30° relative to a reference line parallel to the occlusal plane. The treatment aim was to reduce the inclination from 30° to 5° with the occlusal plane because, according to Andrews' Six Keys of Occlusion, the gingival portion of the tooth is distal to the occlusal portion[18]. The treatment plan required a total uprighting of 25°. The software automatically segmented this movement into 10 stages, each corresponding to a 2.5° increment per aligner.

Five distinct series of aligners were developed, each featuring a different attachment configuration:

1- Control group—no attachment. (Figure 5A&5B)

2- Horizontal rectangular attachment—A single attachment measuring 3 × 2 × 1 mm (length × height × thickness)[19]. (Figure 5C&5D)

3- Alternative twin horizontal attachments—The same horizontal rectangular attachment was divided into two equal parts and spaced 3 mm apart[19]. (Figure 5E&5F).

4- Vertical twin attachments—Two vertical rectangular attachments, each measuring 2 × 3 × 1 mm [20]. (Figure 5G&5H)

5- Inclined attachment—A single rectangular attachment (3 × 2 × 1 mm) placed at a 45° angle to the occlusal plane[21]. (Figure 5I&5J)

Each series of aligners was printed in triplicate (n = 3) to establish sample size. [12] KeyModel resin (Keystone® Industries, USA) was used in conjunction with the Microlay Microlay® Versus 365™ printer, configured to a 100 µm layer thickness. Post-processing followed the same protocol previously described: washing in 96% ethanol for two cycles of 3 minutes using an Anycubic[tm] washer, followed by curing for 10 minutes in the Anycubic[tm] UV chamber[22].

Thermoforming was conducted using CA® Clear Aligner sheets (Scheu-Dental GmbH, Germany) and a Biostar® IV thermoforming unit. The Scheu company recommends using 30s of heating and then 60s of cooling with the initial temperature to achieve the best fitness of the aligner on the 3D-printed models. Then manual trimming and polishing were done on the thermoformed aligners about 2 mm below the gingival line to enhance retention of aligners on the models during the study[23].

Using the Aligners

Maestro 3D™ software (AGE Solutions, Italy) labels the first aligner as the template aligner (T1), which helps to place the attachments on the typodont. After checking the proper fitness of the template on the typodont, a separating medium was applied to the inner surface of the template to facilitate the removal of the template after cutting the attachment composite similarly to protocols in indirect bonding procedures[24]. At the same time, acid etch and bonding were applied to the tooth surface. The attachment cavity within the template was then filled with a PALFIQUE LX5™ (Tokuyama Dental Corp., Japan)[21]. The template was used to transfer the uncured composite onto the typodont, where a curing light was used to cure the material.

Following attachment placement, Aligner No. 1 was fitted onto the typodont. The assembly was then immersed in a water bath at 50°C for 90 seconds, as recommended by the manufacturer of the typodont wax, to allow controlled tooth movement. After immersion, the typodont was removed from the bath and left at room temperature for five minutes to allow for cooling and stabilization of the wax. This thermal cycle was repeated for each subsequent aligner in the series. After application of aligners, a new CBCT was taken to evaluate the movements and new position of the tooth with the reference points.

Statistical Analysis

Data analysis was performed using SPSS® version 25 (IBM Corp., Armonk, NY, USA). Group differences were assessed using the Kruskal–Wallis test, followed by Dunn's post hoc test with Bonferroni correction. Statistical significance was set at $p \leq 0.05$.

Results

For mesiodistal inclination changes, all groups showed different amounts of uprighting capacity, reflecting the attachment geometry. The pretreatment angle between the long axis of the tooth and the reference plane was 60°. The inclined attachment demonstrated the most pronounced effect, 79.5° (78.4°-80°), as in figure 6A, followed by the single horizontal 74.1° (73.2°-74.8°), alternative twin 68.8° (68.4°-69.2°), and twin vertical 64.9° (64.6°-66.1°) groups. The group without attachments, also known as control group, showed least increase, 66.1° (65.7°-66.4°). A Kruskal–Wallis test was done and showed significant difference among groups statistically ($H = 14.03$, $p = 0.015$). Then, a post hoc test was done and revealed that the inclined group was significantly different statistically from the control (adjusted $p = 0.026$), suggesting that this attachment geometry was the most effective in mesiodistal uprighting (see table 1).

For buccolingual inclination, the single horizontal 87.4° (86.4°-88°), inclined 89.5° (86.7°-89.6°), and no-attachment 86.7° (86.3°-87.1°) groups remained close to baseline, whereas the alternative twin 78.2° (75.7°-81.7°), as in figure 6B, and twin vertical 76.1° (74.7°-77.7°) groups exhibited greater buccal tipping. The overall Kruskal–Wallis test showed a significant difference between groups (H = 10.57, p = 0.032), suggesting that twin-type attachments might cause more unwanted movement of the teeth from side to side (see table 1).

Regarding vertical distance, the alternative twin group showed the largest reduction among all the groups 12.3 (12.1-12.4 mm), while the inclined attachment 13 (12.9-13.1 mm), single horizontal 13(12.9-13.35 mm), twin vertical 13 (12.85-13.1 mm), and no-attachment 13.13 (12.9-13.35 mm) groups showed moderate change as in figure 6C.

But the Kruskal–Wallis test showed no significant differences among groups (H = 7.51, p = 0.111) (see table 1).

In terms of mesiodistal distance, the pre-treatment baseline was 15.60 mm. The inclined attachment13.6 (13.4-13.7 mm) and single horizontal 13.73 (13.3-13.8 mm) groups showed the greatest reductions, while the twin vertical 15.27 (15.1-15.5 mm) and alternative twin 14.8 (14.75-15 mm) groups maintained values closer to baseline. The control group showed a mean of 15.07 (15-15.15mm) as in figure 6D. The Kruskal–Wallis test revealed a significant difference across groups (H = 11.39, p = 0.023), although no pairwise comparison remained statistically significant after Bonferroni adjustment (see table 1).

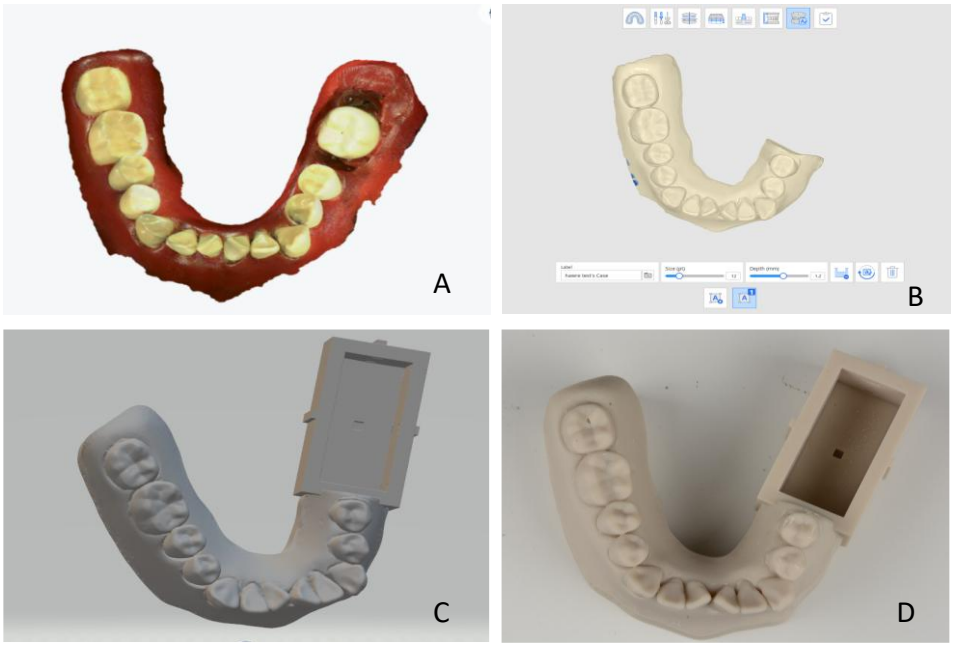

Figure 1: A: First scan of the standard typodont, B: Using Medit model builder to create a model with removing the lower left molar region, C: Virtual typodont after adding supporting box, D: First physical model.

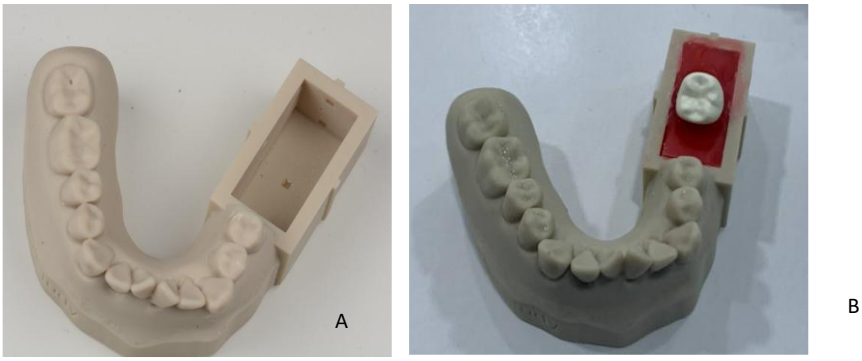

Figure 2: A: Physical model after filling the small cubes with flowable composite, B: Physical model after adding typodont wax and aluminum-based tooth.

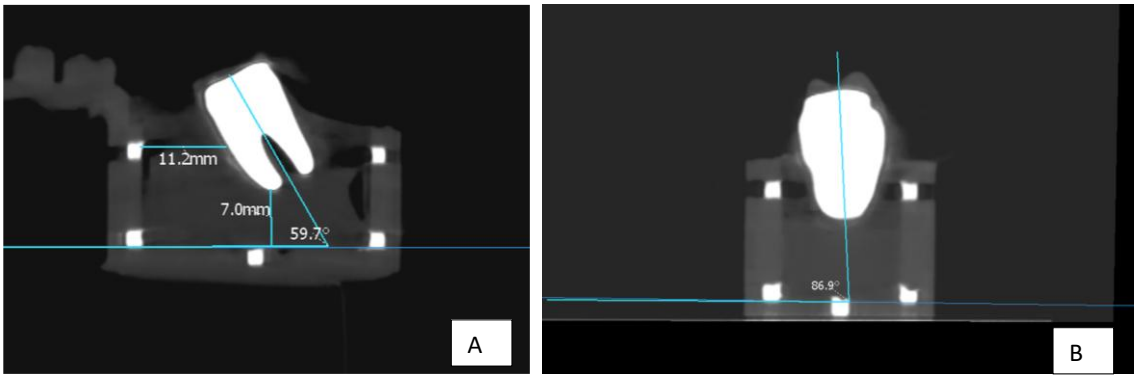

Figure 3: Initial records from CBCT A: Sagittal plane, B: Coronal plane.

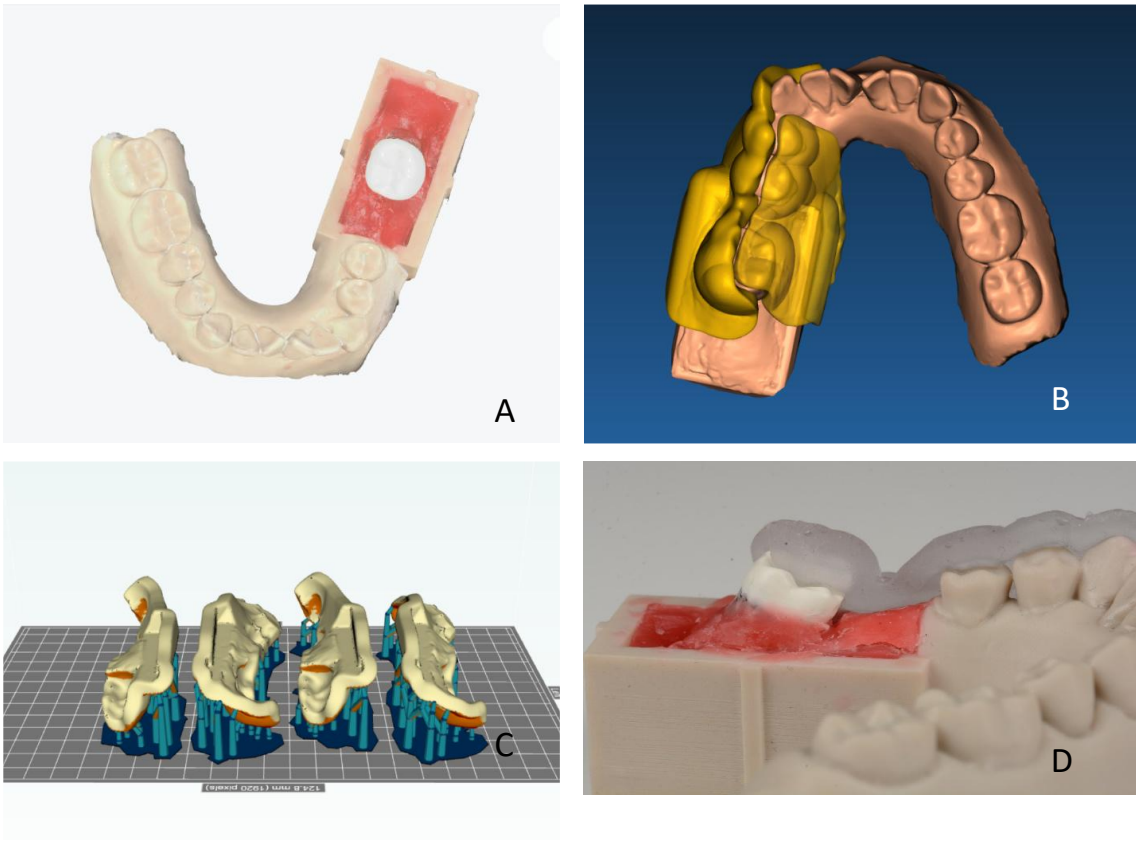

Figure 4: A: OBJ file of first typodont B: Virtual design of guides in REALguide C: Guides ready for print D: Tooth has been placed with help of surgical guide.

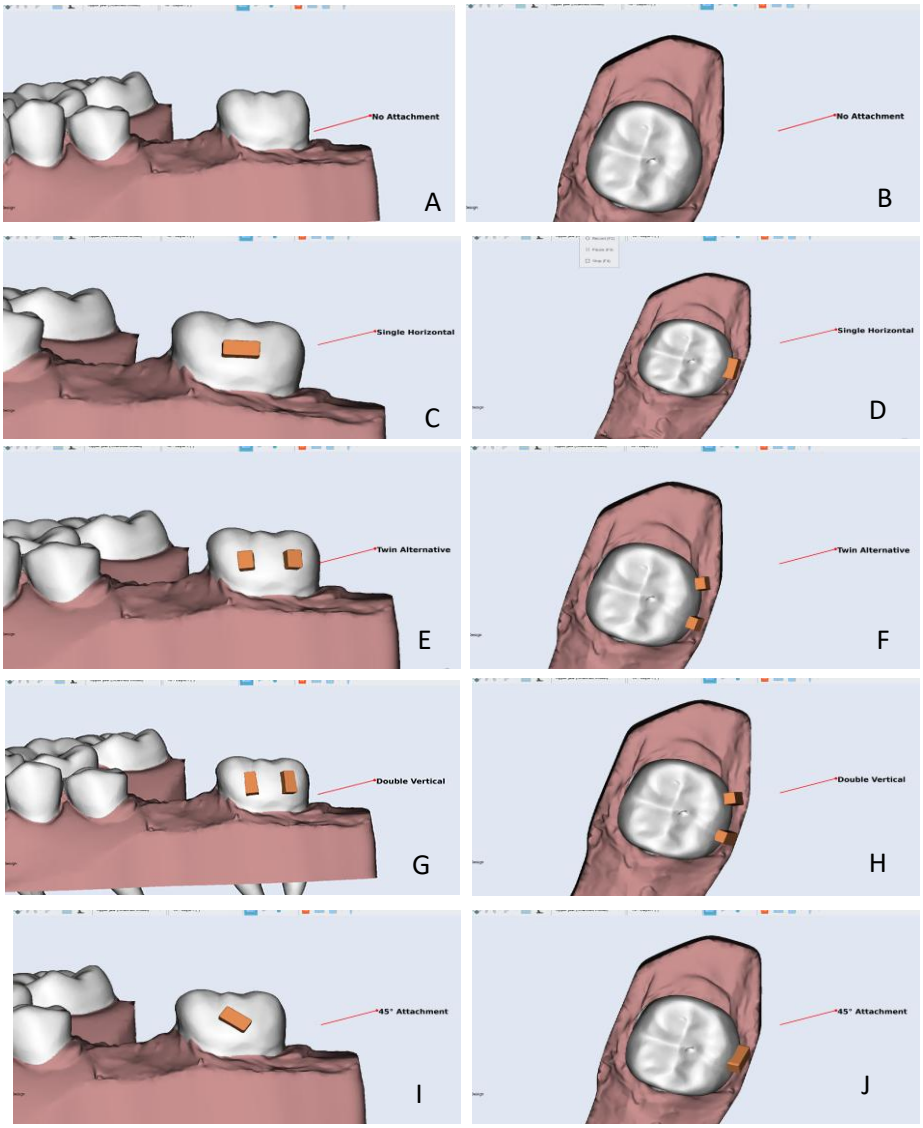

Figure 4: A: Without attachment buccal view, B: Without attachment occlusal view, C: Single horizontal buccal view, D: Single horizontal occlusal view, E: Alternative twin attachments buccal view, F: Alternative twin attachments occlusal view, G: Vertical twin attachments buccal view, H: Vertical twin attachments occlusal view, I: Inclined attachment at 45° to occlusal surface buccal view, L: Inclined attachment at 45° to occlusal surface occlusal view.

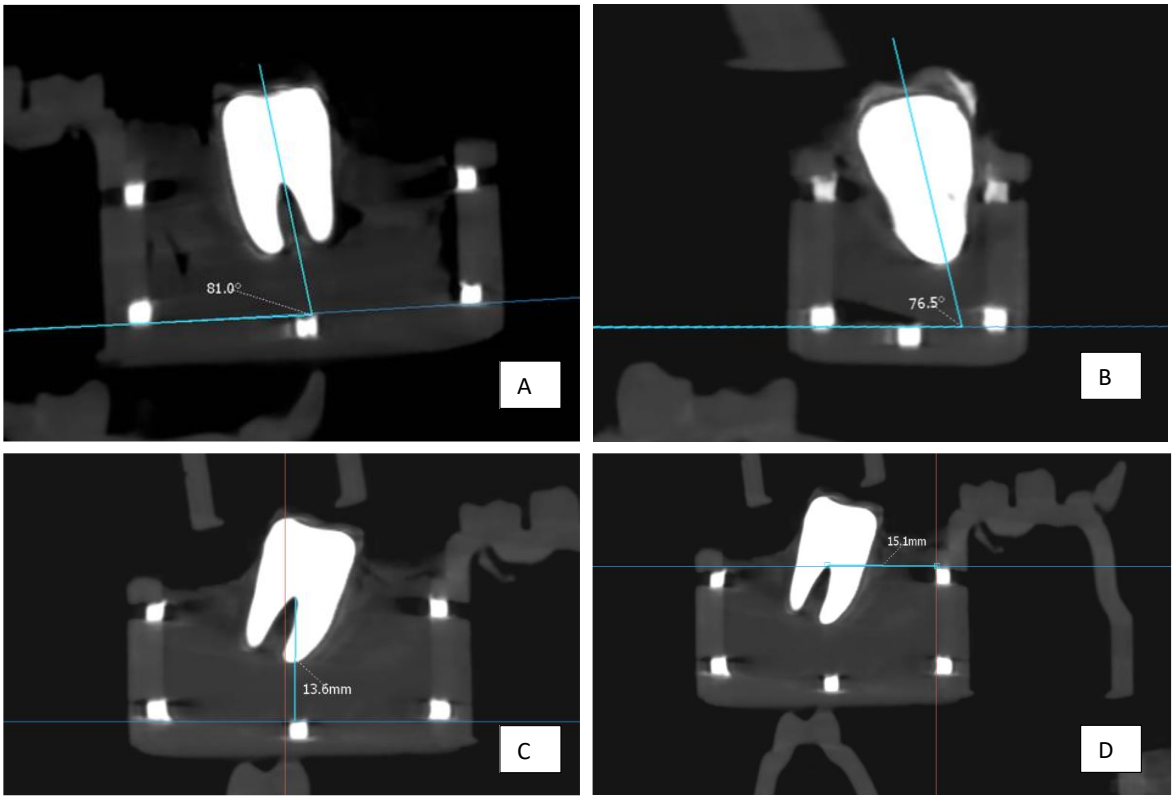

Figure 5: A: Change in mesiodistal inclination by using single oblique rectangular attachment, B: Change in buccolingual inclination by using twin alternative attachment, C: Change in vertical distance in control group(without attachment), D: Change in mesiodistal distance in control group (without attachment).

Table 1: Average change in tooth position.

Type of attachment	**Change in Mesiodistal inclination**		**Change in buccolingual inclination**		**Change in vertical distance**		**Change in mesio-distal distance**	
	Post-test readings	Average change	Post-test readings	Average change	Post-test readings	Average change	Post-test readings	Average change
No attachment	66°	6°	86.7°	0.2°	13.13 mm	1.47 mm	15.07 mm	0.53 mm
Single horizontal rectangle	74°	14°	87.1°	-0.2°	13.00 mm	1.6 mm	13.73 mm	1.87 mm
Inclined attachment	79°	19°	87.9°	-1°	13.27 mm	1.33 mm	13.60 mm	2 mm
Twin alternative	68.8°	8.8°	78.2°	8.7°	12.30 mm	2.3 mm	14.87 mm	0.73 mm
Two vertical rectangular attachments	65.4°	5.4°	76.2°	10.7°	13.00 mm	1.6 mm	15.27 mm	0.33 mm

Discussion

This in vitro study looked into how varied attachment geometries affected the uprighting of second molars in clear aligner therapy. Even though our study has its own limitations, the study showed that simple attachment geometries like single horizontal rectangular and single inclined at 45 degrees to the occlusal plane can act better as compared to complex geometries like alternative twin and double vertical attachments. The findings from the study can help orthodontists and clear aligner technicians to select simple and effective attachments during planning.

The results of this in vitro study showed that single attachments were achieving better results in terms of uprighting a tilted lower second molar as compared to other attachment configurations, like twin vertical and twin horizontal attachments, as well as the control group without attachments. This result shows that the presence of attachments, as well as their shape and direction, are crucial factors in determining how well force is transmitted through clear aligners[21].

One of the reasons why single attachments work better is that they are easier to make and are more likely to contact the aligner material during treatment. A single horizontal attachment gives the force system a wide, uniform surface that makes sure it always makes contact with the aligner. This makes the force system more predictable[25]. Also, a single inclined attachment at 45 degrees to the occlusal plane can make a vector of force that facilitates the efficiency of the attachment to an upright tilted molar by combining horizontal and vertical force components[26].

The less useful twin attachment designs, on the other hand, may be due to several things that affect each other. Constructed complex object shapes like twin attachments are more likely to be inaccurate during the 3D printing and thermoforming steps. Even a small deviation in the attachment's size or location can have a large effect on how well it fits and the direction of force[27]. This is important because thermoforming at high temperatures can cause small changes in the shape and thickness of the material. These small changes in the attachment position and the planned position can add up over the course of treatment and cause a clinically significant error, which leads to poor performance of the attachments[28].

Furthermore, when placing composites, templates with two attachment cavities may not seat properly because they are more rigid or have undercut areas. This makes it harder to make sure that the template fully adapts to the orthodontic appliance or natural teeth. As a result of incomplete seating, attachments may move or become distorted, which makes their effective engagement with the aligner even worse. On the other hand, single attachments are easier to seat correctly because there is less chance of template rocking or incomplete adaptation[29].

From the point of view of biomechanics, single attachments may also make vector distribution simpler. When two attachments are used together, they might create opposing force vectors that hide the original purpose of the vectors at the same time. Twin attachments can also induce torque and moments that tilt the tooth lingually. This could weaken the effective moment arm needed to straighten a tilted molar or lead to off-axis moves that make the force system less effective[26].

In the end, how well the attachment composite and aligner material work together depends on the properties and limitations of both materials. For example, if the attachment composite does not cure properly or bond well to the tooth, it may lead to inaccuracy of fitting and transmitting correct vector of force. In this study, although a nano-hybrid composite (PALFIQUE LX5) was used, even with its outstanding strength, it still can be affected by the angle and strength of the curing light, which make it harder to control when attachments are more complex[27].

Additionally, the thermoforming process itself can be a source of issues affecting the reliability of complex attachment geometries. During this process a heated aligner material is molded onto the 3D-printed models. Complex or large attachments require the thermoplastic to stretch further and conform more to replicate the attachment shape[28]. However, this increased deformation introduces multiple risks. First, the material reduces in thickness, and this localized thinning can reduce the mechanical stiffness of the aligner in critical zones[30]. Second, the sharper the attachment design, the more likely it is to cause material bridging, a phenomenon where the aligner fails to contact the attachment surface fully, creating a void or a gap[31]. Third, increased surface complexity may result in variability in heating and cooling rates across the sheet during thermoforming, which can induce internal stresses and micro-deformations in the material. All these features make it harder for the aligner to fit well with complicated shapes, especially when compared to simpler shapes like single horizontal or inclined attachments. In both clinical and experimental situations, even minor errors in thermoforming can lead

to accumulated inaccuracies in tooth movement, which consequently affects the overall efficacy and predictability of the treatment.

The findings of this study are comparable to those reported in previous research and are consistent with the existing literature[17]. This agreement supports the reliability of the results and indicates that the outcomes are in line with established evidence.

Conclusion

The efficiency of different attachment geometries on uprighting the second molar with clear aligner treatment was assessed using four outcome measures: mesiodistal inclination, buccolingual inclination, vertical distance, and mesiodistal distance. This study supports the idea that simpler attachment shapes are not only easier to make but also more effective in clinical use, as they help apply force more consistently. To better understand these effects, future research could use finite element analysis or in vivo studies to explore how attachment shapes influence molar uprighting in real clinical settings.

References

1. AlMogbel A. Clear Aligner Therapy: Up to date review article. J Orthod Sci. 2023;12(1):37.
2. Rouzi M, Zhang X, Jiang Q, Long H, Lai W, Li X. Impact of clear aligners on oral health and oral microbiome during orthodontic treatment. Int Dent J. 2023;73(5):603-11.
3. Ozmen B. Evaluation of permanent first molar tooth loss in young population from North Turkey. Balk J Dent Med. 2019;23(3):20-3.
4. Rao MH, Aluru SC, Jayam C, Bandlapalli A, Patel N. Molar incisor hypomineralization. J Contemp Dent Pract. 2016;17(7):609-13.
5. Schneider PM, Silva M. Endemic molar incisor hypomineralization: a pandemic problem that requires monitoring by the entire health care community. Curr Osteoporos Rep. 2018;16(3):283–8.
6. Shibasaki WMM, Martins RP. Loads of continuous mechanics for uprighting the second molar on the second molar and premolar. Am J Orthod Dentofacial Orthop. 2022;161(5):679-86.
7. Saber AM, Altoukhi DH, Horaib MF, El-Housseiny AA, Alamoudi NM, Sabbagh HJ. Consequences of early extraction of compromised first permanent molar: a systematic review. BMC Oral Health. 2018;18(1):59.
8. Mahmood TMA. Occlusal plane steepness and profile change following tad-based one-step retraction on four-unit extraction cases: a retrospective study. Diagnostics. 2023;13(14):2395.
9. Magkavali-Trikka P, Emmanouilidis G, Papadopoulos MA. Mandibular molar uprighting using orthodontic miniscrew implants: a systematic review. Prog Orthod. 2018;19(1):1.
10. Bisht S, Khera AK, Raghav P. White spot lesions during orthodontic clear aligner therapy: A scoping review. J Orthod Sci. 2022;11:9.
11. Nucera R, Dolci C, Bellocchio AM, Costa S, Barbera S, Rustico L, et al. Effects of composite attachments on orthodontic clear aligners therapy: a systematic review. Materials. 2022;15(2):533.
12. Rossini G, Parrini S, Castroflorio T, Deregibus A, Debernardi CL. Efficacy of clear aligners in controlling orthodontic tooth movement: a systematic review. Angle Orthod. 2015;85(5):881-9.
13. Yuan X, Liu L, Fan Q, Zhou H, Wang Y, Lai W, et al. Uprighting and protraction of two unilateral mandibular molars using a cantilever arm through a sophisticated biomechanical system with clear aligner: A case report. Int Orthod. 2024;22(3):100893.
14. Ho C-T, Huang Y-T, Chao C-W, Huang T-H, Kao C-T. Effects of different aligner materials and attachments on orthodontic behavior. J Dent Sci. 2021;16(3):1001-9.
15. Rashid ZJ, Chawshli OF. Is bracket position determination from digital techniques accurate 100%?: A omparative ex-vitro study. Eur J Mol Clin Med. 2020;7(1):4384-94.
16. AlKahlan LA, Bindayel NA, Mallek AM, Bendjaballah MZ. Extensive iterative finite element analysis of molar uprighting with the introduction of a novel method for estimating clinical treatment time. Appl Sci. 2025;15(12):6463.
17. Fareed AlSammraaie M, A Fatalla A. The effect of ZrO2 nanoparticles addition on Candida adherence and tensile strength of 3D printed denture base resin. J Nanostructures. 2023;13(2):544-52.
18. Andrews LF. The six keys to normal occlusion. Am J Orthod. 1972;62(3):296-309.
19. Ravindra Nanda, Tommaso Castroflorio, Francesco Garino, Kenji Ojima. PRINCIPLES

and BIOMECHANICS of ALIGNER TREATMENT. first. ELSEVEIR; 2021. 290 p.
20. Mampieri G, Giancotti A. Invisalign technique in the treatment of adults with pre-restorative concerns. Prog Orthod. 2013;14(1):40.
21. Jedliński M, Mazur M, Greco M, Belfus J, Grocholewicz K, Janiszewska-Olszowska J. Attachments for the Orthodontic Aligner Treatment—State of the Art—A Comprehensive Systematic Review. Int J Environ Res Public Health. 2023;20(5):4481.
22. Kirby S, Pesun I, Nowakowski A, França R. Effect of different post-curing methods on the degree of conversion of 3d-printed resin for models in dentistry. Polymers. 2024;16(4):549.
23. Cowley DP, Mah J, O'Toole B. The effect of gingival-margin design on the retention of thermoformed aligners. J Clin Orthod JCO. 2012;46(11):697-702.
24. Hassan MS, Abdelsayed FA, Abdelghany AH, Morse Z, Aboulfotouh MH. For indirect orthodontic attachment placement, adding a custom composite resin base is not beneficial: a split-mouth randomized clinical trial. Scribante A, editor. Int J Dent. 2022;2022(1):9059697.
25. Sultanoğlu E, Gürel HG, Gülyurt M. The effects of different attachment types and positions on rotation movement in clear aligner treatments: a finite element analysis. Cureus. 2024;16(8):1-11.
26. Li J, Yang Y, He X, Lai W, Long H. Effects of attachment orientation and designed vertical movement on molar distalisation with clear aligners: a biomechanical finite element study. Orthod Craniofac Res; 2025;28(2):296-303.
27. Bellocchio AM, Portelli M, Ciraolo L, Ciancio E, Militi A, Peditto M, et al. Evaluation of the clinical variables affecting attachment reproduction accuracy during clear aligner therapy. Materials. 2023;16(20):6811.
28. Elshazly TM, Keilig L, Salvatori D, Chavanne P, Aldesoki M, Bourauel C. Effect of trimming line design and edge extension of orthodontic aligners on force transmission: An in vitro study. J Dent. Elsevier BV; 2022;125:104276.
29. Raluca Fratila C, Alonso-Ezpeleta L, Poveda-Saenz M, Giovannini G, Lobo-Galindo A, Flores-Fraile J, et al. Accuracy evaluation of indirect bonding techniques for clear aligner attachments using 3D-Printed models: an in silico and physical model-based study. Materials. 2025;18(4):780.
30. Elshazly TM, Salvatori D, Elattar H, Bourauel C, Keilig L. Effect of trimming line design and edge extension of orthodontic aligners on force transmission: A 3D finite element study. J Mech Behav Biomed Mater. 2023;140:105741.
31. Park SY, Choi S-H, Yu H-S, Kim S-J, Kim H, Kim KB, et al. Comparison of translucency, thickness, and gap width of thermoformed and 3D-printed clear aligners using micro-CT and spectrophotometer. Sci Rep. Springer Science and Business Media LLC; 2023;13(1):10921.

Original Article

Decisions in Restorative Dentistry Based on Gender, Knowledge, and Experience

Hawzhen M. Mohammed[1], *Sara H. Kazzaz* [1], *Dlsoz O. Babarasul*[1], *Didar S. Hama Gharib*[1*], *Darwn S. Abdulateef*[1]

Abstract

Objective: The increasing emphasis on esthetic outcomes and patient-centered care has significantly shaped clinical decisions in restorative dentistry. This study investigates how dentists' knowledge and professional experience influence treatment choices in various restorative scenarios.

Methods: A questionnaire was distributed to general dentists and specialists in Kurdistan Region of Iraq. It assessed treatment choices in restorative scenarios and gathered demographic data. Statistical analysis examined links between clinical decisions and factors like gender, experience, and specialization.

Results: The results revealed significant differences in treatment choices based on gender and experience. Male dentists were more likely to choose root canal therapy and place posts, while females showed a greater tendency toward conservative treatment options. More experienced dentists preferred full crowns for severely damaged teeth, whereas less experienced ones were more likely to opt for direct restorations. Additionally, most practitioners discussed esthetic decisions, such as veneer shade, with patients, and the majority favored implants over bridges for replacing missing teeth.

Conclusions: These findings highlight the influence of demographic and professional characteristics on clinical decision-making in restorative dentistry. Knowledge, and experience contribute to differing approaches in treatment planning, reflecting a balance between technical knowledge and evolving trends in patient-centered, esthetically driven care.

Keywords: *Clinical decision-making; Dentist experience; Esthetic dentistry; Gender differences; Patient-centered care; Restorative dentistry.*

Submitted: October 5, 2025, Accepted: November 13, 2025, Published: December 1, 2025.

Cite this article as: Mohammed HM, Kazzaz SH, Babarasul DO, Hama Gharib DS, Abdulateef DS. Decisions in Restorative Dentistry Based on Gender, Knowledge, and Experience. Sulaimani Dent J. 2025;12(3):42-50.

DOI: https://doi.org/10.17656/sdj.10215

1. *Department of Operative Dentistry and Endodontics, College of Dentistry, University of Sulaimani, Sulaimani, Iraq.*

* *Corresponding author*: *didar.hamagharib@univsul.edu.iq.*

Introduction

Clinical decision-making is at the core of dental practice, influencing treatment choices that impact long-term patient outcomes. In restorative dentistry, these decisions require a balance between scientific evidence, clinical expertise, and patient preferences. Dental professionals who have acquired information and possess a sense of autonomy over their oral health are more inclined to engage in self-care practices[1].

Medical decision-making in healthcare has evolved from a physician-centered approach to a more collaborative process, integrating patient preferences and clinical expertise[2]. This shift is particularly relevant in dentistry, where treatment outcomes depend on both functional and aesthetic considerations[3]. Shared decision-making (SDM) plays a crucial role in this process by ensuring that evidence-based recommendations align with patient expectations, leading to more informed and personalized treatment plans[2,3]. However, applying evidence-based dentistry in daily practice is not without challenges. Dentists often face difficulties in applying standardized guidelines because of financial constraints, differences in training, and patient demands[4,5]. These factors contribute to a persistent gap between evidence-based recommendations and actual clinical practice, leading to inconsistencies in treatment decisions[5,6]. Bridging this gap requires stronger integration of research findings into daily dental care[6,7]. Insurance policies and treatment costs often dictate which procedures are prioritized, making it difficult for dentists to consistently apply evidence-based guidelines, particularly in private practice settings[8].

The amount of residual structure, the crown-to-root ratio, and the material selection all affect tooth restorability; these factors showed how knowledge and experience guide restorative dentistry decisions. Implants and extraction might be preferable if insufficient. It was found that the study participants were eager to choose dental implants but were restricted due to financial issues[9]. When possible, root canal therapy is recommended; nevertheless, its success is influenced by patient characteristics, infection management, and prognosis. Additionally sufficient tooth structure and periodontal support are necessary for crowns[10].

Experienced dentists prioritize conservative, functional treatments, while less experienced ones may opt for quicker, irreversible options. Balancing aesthetics, patient demands, and professional judgment is key; however, commercialization is increasingly influencing dentistry[11]. Furthermore, rather than being motivated by health or scientific rationale, patients' perceptions of facial beauty and aesthetic dental appearance (Hollywood smile makeover) are now influenced by the beauty exhibited by movie actors and social media influences[12].

When making treatment decisions, good clinical practice relies on the capacity to integrate evidence-based knowledge, reflect on prior experiences, and apply these to a clinical situation. First, the decision-making process – whether to replace or restore – is difficult. Second, various methods have been developed to help less experienced physicians, and attempts have been made to rationalize the procedure. As demonstrated by studies that have looked at the treatment planning of people with different clinical backgrounds and experiences, challenges still exist despite these efforts[13].

This study aims to evaluate how dentists make decisions regarding the treatment choices presented to the patient and these are gender, years of experience, the country where they obtained their degree, and their training status. Through the structured questionnaire that was presented to many dentists in the field, patterns of decision-making relating to restorative dentistry will be analyzed.

Materials and methods

The questionnaire used in this study was adapted from previously validated research conducted by Al-Asmar et al., with modifications made by the Department of Operative Dentistry and Endodontics, College of Dentistry, University of Sulaymaniyah, to reflect local clinical practices and current evidence-based treatments[14]. The survey was distributed online via Instagram, WhatsApp, Messenger, and Viber over a three-month period (October 2024 to January 2025) and targeted general practitioners with at least two years of experience as well as specialists in restorative dentistry (operative dentistry, endodontics, and fixed prosthodontics). Power analysis was performed using G*Power version 3.1. Assuming a moderate effect size (Cohen's $w = 0.25$), an $\alpha = 0.05$, and a power = 0.80 for a Chi-square test with the groups, the minimum required sample size was 126 participants. The current study included 166 dentists, which exceeds this requirement and provides adequate statistical power to detect meaningful associations.

Ethical approval was granted by the Ethical Committee of the College of Dentistry, University of Sulaimani, Sulaimaniyah, Iraq (No. 239/24, dated December 16, 2024).

Content validity was ensured through expert review by faculty members in restorative dentistry, assessing the relevance, clarity, and comprehensiveness of the items. Face validity was evaluated through pilot testing with 10 dentists who were not included in the main study, leading to minor adjustments for clarity.

Construct validity was established by organizing the questionnaire into distinct domains, including demographic characteristics, professional experience, and clinical treatment preferences. The following questions were posed to the dentist:

1- Management of teeth diagnosed with irreversible pulpitis:

Which treatment approach do you most commonly prefer?

A- Vital pulp therapy (if applicable)

B- Root canal treatment (as best predictable successful treatment)

2- Use of posts in endodontically treated teeth:

Do you routinely place a post in endodontically treated teeth for protection, regardless of the remaining tooth structure or other factors?

A- Yes

B- No

3- Full coverage after root canal treatment:

Do you routinely place a full-coverage crown after root canal treatment, regardless of the amount of remaining tooth structure?

A- Yes

B- No

4- Management of patients requesting a "Hollywood smile" or smile makeover:

When a patient requests a Hollywood smile or aesthetic smile enhancement, which of the following best describes your approach?

A- I offer him/her porcelain/ceramic veneers on the upper or/and lower anterior teeth as it is the first choice of treatment in such conditions.

B- I offer him/her other choices such as bleaching, orthodontic treatment, and/or dental composite veneering

C- I offer no treatment at all if unnecessary

5- Shade selection for anterior veneers:

When selecting the shade for anterior veneers, which approach do you typically follow?

A- I choose the color (shade) according to the clinical condition of my patient.

B- I let my patients choose the color (shade)

C- I discuss the color (shade) with my patients, and I convince them of the best, despite his/her preference.

6- Treatment of badly damaged teeth:

How do you generally manage teeth with severe structural damage?

A- Direct restoration with composite or amalgam

B- Intra-coronal restorations (inlays/onlays)

C- Full cuspal coverage (full crowns)

D- Extraction and implant placement.

7- Replacement of missing teeth:

When recommending replacement of a missing tooth, what is your usual first-line treatment option?

A- An implant is the first choice of treatment

B- A dental bridge

Statistical analysis

Data were entered into SPSS version 26 (IBM Corp., Armonk, NY, USA) for analysis. Descriptive statistics were used to summarize demographic and professional characteristics (frequencies, percentages, means, and standard deviations). Comparisons were performed using the Chi-square test for categorical variables. P-values < 0.05 were regarded as statistically significant.

Results

The questionnaire was answered by 166 dentists (89 males [53.6%] and 77 females [46.4%]). Table 1 represents the demographic characteristics of the study population.

As indicated in Table 2, the study assessed the preferences of male and female dental professionals regarding various dental treatments. The majority of dentists (84.3%) favored root canal treatment over vital pulp therapy (15.7%) for cases of irreversible pulpitis, with a stronger preference for root canal treatment

among male dentists, while female dentists tended to perform vital pulp therapy more frequently. This showed a significant difference (p=0.029). In terms of root canal-treated teeth, 27.1% of dentists routinely placed a post regardless of the condition of the remaining tooth structure. This procedure was more prevalent among male dentists (33.7%) compared to female dentists (19.5%), indicating a significant difference (p = 0.04). Furthermore, most dentists routinely did not place crowns on all root canal-treated teeth for protection, regardless of the remaining tooth structure, and there were no significant differences observed when treating significantly damaged teeth with full crowns. When performing anterior veneering and Hollywood smile procedures, a majority preferred to provide no treatment when asked by the patient (42.2%) and discussed shade options with their patients (68.6%). Dental implants emerged as the preferred treatment choice for patients with missing teeth.

The data revealed differences in treatment preferences based on clinicians' experience, as summarized in Table 3. Most practitioners preferred root canal treatment for irreversible pulpitis, showing no significant variability. After root canal treatment, the rates of post and crown placement were consistent across all groups. Full crowns were the preferred choice (53.6%), although less experienced dentists tended to use more direct restorations (22.9%) for severely damaged teeth, showing a significant difference (p = 0.04). Additionally, most practitioners adopted a more conservative approach when patients requested a Hollywood smile by opting for unnecessary treatments. Concerning veneer shade selection, 68.6% of dentists engaged in discussions with their patients about this aspect. This practice was notably more common among those with 11-20 years of experience compared to others, revealing a significant difference (p = 0.01). Despite less experienced dentists showing a slight preference for bridges over implants (11.5%), implants remained the favored choice for addressing missing teeth (90.4%).

Table 1: Socio-demographic characteristics of the studied sample.

Variables		**n (%)**
Gender	Male	89(53.6)
	Female	77(46.4)
Years of experiences	<5	61(36.7)
	5-10	57(34.3)
	11-20	39(23.5)
	>20	9(5.4)
Training status	General practitioner	122(73.5)
	Specialist (Conservative dentistry)	21(12.7)
	Specialist (Endodontic)	7(4.2)
	Specialist (Prosthodontic)	16(9.6)
Working place	Private clinic	127(76.5)
	University	20(12)
	Ministry of Health	18(10.8)
	Other	1(0.6)

n: number of the variables, %: percentage

Table 2: Analysis of questionnaire responses based on gender.

Condition	Treatment options	Total %	Gender		*P- value*
			Male	Female	
Irreversible pulpitis	Vital pulp therapy	15.7	22	36	**0.029**
	RCT	84.3	78	64	
Post for root canal treated teeth	Yes	27.1	33.7	19.5	**0.04**
	No	72.9	66.3	80.5	
Crown any tooth after RCT	Yes	21.7	19.1	24.7	**0.38**
	No	78.3	80.9	75.3	
Badly damaged teeth	Composite or amalgam	12	13.5	10.4	**0.29**
	Inlays/onlays	19.9	24.7	14.3	
	Full crowns	53.6	48.3	59.7	
	Extraction and implant	14.5	13.5	15.6	
Hollywood smile or smile makeover	I offer porcelain/ceramic veneers	12.7	12.4	12.9	**0.4**
	I offer bleaching	39.8	35.9	44.2	
	Dental composite veneering	5.3	7.9	2.6	
	I offer no treatment	42.2	43.8	40.3	
Anterior veneers	I choose the color (shade) according to the clinical condition	17.5	22.5	11.7	**0.18**
	I let my patients choose the color (shade)	13.9	12.4	15.6	
	I discuss the color (shade) with my Patients	68.6	65.1	72.7	
Restoring missing tooth	An implant as first choice of treatment	90.4	88.8	92.2	**0.45**
	A bridge	**9.6**	**11.2**	**7.8**	

P-value; significant level (P<0.05).

Table 3: Analysis of questionnaire responses based on years of experience.

Condition	Treatment options	Total %	Experience (years)				*P- value*
			<5	5–10	11–20	>20	
Irreversible pulpitis	Vital pulp therapy	15.7	23	12.3	7.7	22.2	**0.16**
	RCT	84.3	77	87.7	92.3	77.8	
Post for root canal treated teeth	Yes	27.1	26.2	26.3	25.6	44.4	**0.69**
	No	72.9	73.8	73.7	74.4	55.6	
Crown any tooth after RCT	Yes	21.7	21.3	24.6	15.4	33.3	**0.59**
	No	78.3	78.7	75.4	84.6	66.7	
Treat badly damaged teeth	Composite or amalgam	12	22.9	7	5.1	0	**0.04**
	Inlays/onlays	19.9	14.8	28.1	15.4	22.2	
	Full crowns	53.6	54.1	49.1	56.4	66.7	
	Extraction and implant placement	14.5	8.2	15.8	23.1	11.1	
Hollywood smile or smile makeover	I offer porcelain/ceramic veneers	12.7	9.8	12.3	15.4	22.2	**0.72**
	I offer bleaching	39.8	34.4	43.9	41	44.4	
	Dental composite veneering	5.3	4.9	8.8	2.6	0	
	I offer no treatment	42.2	50.8	35.1	41	33.3	
Anterior veneers	I choose the color (shade) according to the clinical condition	17.5	23	10.5	10.3	55.6	**0.01***
	I let my patients choose the color (shade)	13.9	14.8	17.5	7.7	11.1	
	I discuss the color (shade) with my patients	68.6	62.2	72	82	33.3	
Restoring missing tooth	An implant as first choice of treatment	90.4	88.5	93	89.7	88.9	**0.87**
	A bridge	**9.6**	**11.5**	**7**	**10.3**	**11.1**	

*; indicate significant, *P-value*; significant level (P<0.05).

Discussion

The data that support the findings of this study are available from the corresponding author upon reasonable request.

The decision-making process in restorative dentistry is deeply influenced by both the clinical knowledge and professional experience of the dentist. These two factors play a critical role in treatment planning, material selection, and long-term prognosis of restorations. Experienced practitioners tend to rely not only on evidence-based guidelines but also on refined clinical judgment developed through years of hands-on practice.

The majority of dentists favored root canal therapy (RCT) over vital pulp therapy (VPT), with male dentists

exhibiting a stronger preference for RCT compared to female dentists, who demonstrated a larger inclination towards VPT. Additionally, the present investigation revealed that males exhibited a greater propensity for consistently placing posts during root canal treatment. This discovery, which corresponds with Al Faisal Y et al., indicates that female practitioners prefer less invasive procedures compared to male practitioners[15]. Additionally, Alfaisal Y et al. state that female, more experienced dentists and endodontists showed greater preference for VPT for irreversible pulpitis in comparison to other participants. In contrast, Mohammad Alwadani et al. observed no significant gender differences in treatment preferences for irreversible pulpitis and state that both male and female dentists and dental interns preferred RCTs with restorations over extraction and implants in the anterior teeth, both with and without prior RCTs, according to the current survey[16]. Meanwhile, Mannocci F et al. found, regarding post placement, that root canal posts primarily provide retention for the coronal restoration of substantially compromised root filled teeth. Even with the improvement of adhesive luting techniques, the contribution to the stability of the root by adhesively placed root canal posts remains questionable and these are predominantly considered for the restoration of weakened traumatized maxillary anterior teeth with thin dentinal walls[17].

This study indicates that the majority of dentists do not consistently fit crowns following root canal therapy. Motasum Abu-Awwad stated that the vast majority of participants (95%) concluded that vital teeth with an occlusal cavity and a residual axial wall thickness of ≥2 mm did not require cuspal covering, which corresponds with our finding[18].

Sequeira-Byron P et al. discovered no clear difference between the crown and composite group and the composite only group in failures of the restoration in their study on composite restored teeth versus indirectly restored teeth with crown[19]. On the other hand, Durre Sadaf concluded that the crown should be placed as soon as possible because delay in crown placement has potentially significant negative impact on endodontically treated teeth survival[20].

Dentists possessing more than 20 years of experience favored complete crowns, in accordance with Al-Asmar AA et al. concluded that regarding the restorative procedures, clinical decision-making in dental practice is highly influenced by the clinician's own knowledge background and clinical experience. Additionally, they observed that 72% of their surveyed dentists treated badly damaged teeth with full crowns, while prosthodontics specialists used inlays/onlay more frequently[21].

Dentists may offer patients conservative, efficient, and patient-centred care by adopting the concepts of minimally invasive dentistry and incorporating developments in materials and technology[22]. Rosenberg, however, contends that porcelain veneers are better than bleaching for long-term cosmetic results, which runs counter to the predilection for bleaching over veneers. He claims that although bleaching might temporarily whiten teeth, porcelain veneers outlast bleaching or composite veneers by remaining essentially stain-free and bright for around 15 years. According to the report, skilled cosmetic dentists frequently discover that veneers offer a more thorough smile makeover by addressing shape, contour, and harmony in addition to colour – achievable with bleaching alone. Additionally, the study mentions that bleaching necessitates multiple treatments, which over time makes veneers more practical and economical even though they initially cost more[22].

Shade selection for anterior veneers is a critical component of aesthetic dentistry, and the approach to this task can be influenced by the clinician's level of experience. More experienced dentists tend to involve patients more actively in the decision-making process, discussing various shade options and considering individual preferences and facial characteristics to achieve optimal aesthetic outcomes. This trend is supported by Kim et al., who found that clinicians with more years of practice were significantly more likely to consult patients about shade preferences and utilize a broader range of shade-matching techniques. Experienced practitioners also reported greater confidence in selecting shades without solely relying on standardized shade guides[23]. In contrast, a study by Lee and Park found that shade selection practices did not differ significantly between experienced and less experienced clinicians. Their findings suggest that adherence to formal training protocols and the increasing availability of objective shade-matching technologies contribute to consistent practices across different experience levels. Together, these findings indicate that while clinical experience may enhance communication and confidence, structured training plays a key role in ensuring uniformity in shade selection procedures[24].

There appears to be a noticeable preference among dental practitioners for using dental implants rather than traditional bridges when replacing missing teeth. A significant proportion of dentists indicated that they favored implants as the more suitable and durable option, with this trend being especially prominent among female dentists (92.2%) and those who had been practicing for between five and ten years (93%). This pattern suggests that both gender and years of clinical

experience may influence restorative treatment preferences. The findings of Johnson et al. support this observation, as their study demonstrated a statistically significant inclination towards implant-supported restorations within these specific subgroups[25]. In contrast, Smith and Allen reported conflicting results, finding no substantial variation in preference based on gender or years of experience[26]. Their study suggested that individual clinical judgment and patient-specific factors may play a more dominant role in treatment decisions than demographic characteristics alone. This divergence in findings highlights the complexity of clinical decision-making in restorative dentistry and suggests a need for further research to clarify the factors that most strongly influence the choice between implants and bridges.

This study was based on self-reported questionnaire data, which may not fully reflect actual clinical practices. The sample was limited to a specific geographic region, potentially affecting the generalizability of the findings. Furthermore, the cross-sectional design restricts the ability to determine causal relationships between demographic factors, clinical experience, and treatment preferences. Future research should include larger and more diverse populations, employ longitudinal or observational study designs, and incorporate qualitative approaches to better understand the factors influencing dentists' clinical decision-making in restorative and endodontic treatments.

Conclusion

The majority of dentists demonstrated a clear preference for root canal therapy over vital pulp therapy in the management of irreversible pulpitis, with male practitioners exhibiting a stronger inclination toward RCT and female dentists showing a greater tendency toward VPT. Clinical experience, professional specialization, and practice setting influenced treatment choices, particularly regarding post and crown placement following RCT. Preferences for aesthetic treatments differed, with numerous practitioners advocating for conservative methods. Dental implants were consistently identified as the preferred option for tooth replacement, and most practitioners emphasized shared decision-making through patient involvement in veneer shade selection. Overall, the findings highlight that gender, experience, and specialty training play significant roles in shaping clinical decision-making in restorative and endodontic practice.

Acknowledgments

The authors would like to express their sincere appreciation to **Lara Alan Saeed, Gash Barham Jamal, Sima Hawre Hussein, Zhina Hassan Hama, Ziad Kamil Tawfeeq, Ahmad Faruq Wahab, Mohammad Abid Arif, Zanyar Mutalib Ibrahim, Ahmad Sherzad Izzat, and Hede Hassan Ali** for their valuable support and assistance throughout various stages of this research. Their contributions were instrumental to the successful completion of this study.

References

1. Noori AJ. Oral health behaviours, knowledge and attitudes among dental college students in Sulaimani city, Iraq. Sulaimani Dent J. 2021;8(1):8-16.
2. Elwyn G, Frosch D, Thomson R, Joseph-Williams N, Lloyd A, Kinnersley P, et al. Shared decision making: a model for clinical practice. J Gen Intern Med. 2012;27(10):1361-7.
3. Kay E, Vascott D, Hocking A, Nield H. Principles of shared decision-making in dentistry. Br Dent J. 2017;222(3):185-90.
4. Richards D. Evidence-based dentistry: Part 1. Getting started. Br Dent J. 2004;196(1):35-9.
5. Straub-Morarend CL, Marshall TA, Holmes DC, Finkelstein MW. Toward defining dentists' evidence-based practice: influence of culture, attitudes, and perceptions. J Dent Educ. 2016;80(9):1032-40.
6. Schwendicke F, Frencken JE, Bjørndal L, Maltz M, Manton DJ, Ricketts D, et al. Managing carious lesions: consensus recommendations on carious tissue removal. Adv Dent Res. 2016;28(2):58-67.
7. Yamalik N, Ensaldo-Carrasco E, Bourgeois D, Ortiz-Magro H, Williams DM. Patient safety and dentistry: what do we need to know and do? Int Dent J. 2020;70(6):507-19.
8. Manski RJ, Moeller JF, Chen H. Dental care coverage and use: modeling limitations and policy implications. Am J Public Health. 2014;104(5):e83-9.
9. Amin NAM. Perception, sentiments, and the level of awareness toward the dental implant among general population in Sulaimaniyah City, Iraq. BMC Oral Health. 2024;24(1):255.
10. Rosen E NCTI. Evidence-Based Decision Making in Dentistry. Rosen E, Nemcovsky CE,

Tsesis I, editors. Cham: Springer International Publishing; 2017. 7-9 p.
11. Rosen E NCTI. Strategic value of the tooth and treatment. In: Evidence-based decision making in dentistry: multidisciplinary management of the natural dentition. Springer International Publishing. Springer International Publishing; 2017. 53-5 p.
12. Ansari SH, Alzahrani AAA, Abomelha AMS, Elhalwagy AEA, Alalawi TNM, Sadiq TWM. Influence of social media towards the selection of Hollywood smile among the university students in Riyadh City. J Family Med Prim Care. 2020;9(6):3037-41.
13. Banerjee A. Minimum intervention oral healthcare delivery-is there consensus? Br Dent J. 2020;229(7):393-5.
14. Al-Asmar AA, Al-Hiyasat AS, Abu-Awwad M, Mousa HN, Salim NA, Almadani W, et al. Reframing Perceptions in Restorative Dentistry: Evidence-Based Dentistry and Clinical Decision-Making. Int J Dent. 2021 Dec 31;2021:1-10.
15. Alfaisal Y, Idris G, Peters OA, Peters CI, Zafar S. Factors influencing treatment decisions in permanent mature teeth with irreversible pulpitis: a questionnaire-based study. Aust Dent J. 2024;69(4):293-303.
16. Alwadani M, Mashyakhy MH, Jali A, Hakami AO, Areshi A, Daghriri AA, et al. Dentists and dental intern's preferences of root canal treatment with restoration versus extraction then implant-supported crown treatment plan. Open Dent J. 2019;13(1):93-100.
17. Mannocci F, Bitter K, Sauro S, Ferrari P, Austin R, Bhuva B. Present status and future directions: the restoration of root filled teeth. Int Endod J. 2022;55(4):1059-84.
18. Abu-Awwad M. Dentists' decisions regarding the need for cuspal coverage for endodontically treated and vital posterior teeth. Clin Exp Dent Res. 2019;5(4):326-35.
19. Sequeira-Byron P, Fedorowicz Z, Carter B, Nasser M, Alrowaili EF. Single crowns versus conventional fillings for the restoration of root-filled teeth. Cochrane Database Syst Rev. 2015;2015(9):CD009109.
20. Sadaf D. Survival rates of endodontically treated teeth after placement of definitive coronal restoration: 8-year retrospective study. Ther Clin Risk Manag. 2020;125-31.
21. Al-Asmar AA, Al-Hiyasat AS, Abu-Awwad M, Mousa HN, Salim NA, Almadani W, et al. Reframing perceptions in restorative dentistry: evidence-based dentistry and clinical decision-making. Int J Dent. 2021;2021(1):4871385.
22. Rosenberg JM. Minimally invasive dentistry: a conservative approach to smile makeover. Compend Contin Educ Dent. 2017;38(1):38-42.
23. Almansour MI, Madfa AA, Alrashid SA, Altuwayhir DA, Alshammari AM, Alfhaed NK. Knowledge and awareness of tooth shade selection principles among senior dental students, interns, and general dentists of Hail Province of Saudi Arabia. Open Dent J. 2023;17(1):1-9.
24. Lee JH, Kim HK. A comparative study of shade-matching performance using intraoral scanner, spectrophotometer, and visual assessment. Sci Rep. 2024;14(1):23640.
25. Levin L, Halperin-Sternfeld M. Tooth preservation or implant placement: a systematic review of long-term tooth and implant survival rates. J Am Dent Assoc. 2013;144(10):1119-33.
26. Alalawi H, Alhumaily H. Professional assessment compared to patients' attitudes toward tooth replacement: a cross-sectional study. BMC Oral Health. 2023;23(1):634.